



TECH BRIEFS

NATIONAL AERONAUTICS AND SPACE ADMINISTRATION

-  **Technology Focus**
-  **Electronics/Computers**
-  **Software**
-  **Materials**
-  **Mechanics**
-  **Machinery/Automation**
-  **Manufacturing & Prototyping**
-  **Bio-Medical**
-  **Physical Sciences**
-  **Information Sciences**
-  **Books and Reports**

INTRODUCTION

Tech Briefs are short announcements of innovations originating from research and development activities of the National Aeronautics and Space Administration. They emphasize information considered likely to be transferable across industrial, regional, or disciplinary lines and are issued to encourage commercial application.

Availability of NASA Tech Briefs and TSPs

Requests for individual Tech Briefs or for Technical Support Packages (TSPs) announced herein should be addressed to

National Technology Transfer Center

Telephone No. (800) 678-6882 or via World Wide Web at www2.nttc.edu/leads/

Please reference the control numbers appearing at the end of each Tech Brief. Information on NASA's Innovative Partnerships Program (IPP), its documents, and services is also available at the same facility or on the World Wide Web at <http://ipp.nasa.gov>.

Innovative Partnerships Offices are located at NASA field centers to provide technology-transfer access to industrial users. Inquiries can be made by contacting NASA field centers listed below.

NASA Field Centers and Program Offices

Ames Research Center

Lisa L. Lockyer
(650) 604-1754
lisa.l.lockyer@nasa.gov

Dryden Flight Research Center

Gregory Poteat
(661) 276-3872
greg.poteat@dfrc.nasa.gov

Goddard Space Flight Center

Nona Cheeks
(301) 286-5810
nona.k.cheeks@nasa.gov

Jet Propulsion Laboratory

Ken Wolfenbarger
(818) 354-3821
james.k.wolfenbarger@jpl.nasa.gov

Johnson Space Center

Michele Brekke
(281) 483-4614
michele.a.brekke@nasa.gov

Kennedy Space Center

Jim Aliberti
(321) 867-6224
Jim.Aliberti@nasa.gov

Langley Research Center

Martin Waszak
(757) 864-4052
martin.r.waszak@nasa.gov

Glenn Research Center

Robert Lawrence
(216) 433-2921
robert.f.lawrence@nasa.gov

Marshall Space Flight Center

Vernotto McMillan
(256) 544-2615
vernotto.mcmillan@msfc.nasa.gov

Stennis Space Center

John Bailey
(228) 688-1660
john.w.bailey@nasa.gov

Carl Ray, Program Executive

Small Business Innovation
Research (SBIR) & Small
Business Technology
Transfer (STTR) Programs
(202) 358-4652
carl.g.ray@nasa.gov

Merle McKenzie

Innovative Partnerships
Program Office
(202) 358-4652
merle.mckenzie-1@nasa.gov



TECH BRIEFS

NATIONAL AERONAUTICS AND SPACE ADMINISTRATION



5 Technology Focus: Sensors

- 5 Airport Remote Tower Sensor Systems
- 6 Implantable Wireless MEMS Sensors for Medical Uses
- 6 Embedded Sensors for Measuring Surface Regression
- 7 Coordinating an Autonomous Earth-Observing Sensorweb
- 8 Range-Measuring Video Sensors
- 9 Stability Enhancement of Polymeric Sensing Films Using Fillers
- 10 Sensors for Using Times of Flight To Measure Flow Velocities



11 Electronics/Computers

- 11 Receiver Would Control Phasing of a Phased-Array Antenna
- 12 Modern Design of Resonant Edge-Slot Array Antennas
- 13 Carbon-Nanotube Schottky Diodes
- 14 Simplified Optics and Controls for Laser Communications
- 14 Coherent Detection of High-Rate Optical PPM Signals
- 15 Multichannel Phase and Power Detector



17 Software

- 17 Using Satellite Data in Weather Forecasting: I
- 17 Using Dissimilarity Metrics To Identify Interesting Designs
- 17 X-Windows PVT Widget Class
- 17 Shuttle Data Center File-Processing Tool in Java
- 17 Statistical Evaluation of Utilization of the ISS



19 Materials

- 19 Nanotube Dispersions Made With Charged Surfactant
- 19 Aerogels for Thermal Insulation of Thermoelectric Devices

- 20 Low-Density, Creep-Resistant Single-Crystal Superalloys



23 Mechanics

- 23 Excitations for Rapidly Estimating Flight-Control Parameters
- 24 Estimation of Stability and Control Derivatives of an F-15
- 25 Tool for Coupling a Torque Wrench to a Round Cable Connector



27 Machinery/Automation

- 27 Ultrasonically Actuated Tools for Abrading Rock Surfaces
- 27 Active Struts With Variable Spring Stiffness and Damping



29 Bio-Medical

- 29 Multiaxis, Lightweight, Computer-Controlled Exercise System
- 30 Dehydrating and Sterilizing Wastes Using Supercritical CO₂



31 Physical Sciences

- 31 Alpha-Voltaic Sources Using Liquid Ga as Conversion Medium
- 31 Ice-Borehole Probe
- 33 Alpha-Voltaic Sources Using Diamond as Conversion Medium
- 33 White-Light Whispering-Gallery-Mode Optical Resonators



35 Books & Reports

- 35 Controlling Attitude of a Solar-Sail Spacecraft Using Vanes
- 35 Wire-Mesh-Based Sorber for Removing Contaminants From Air

This document was prepared under the sponsorship of the National Aeronautics and Space Administration. Neither the United States Government nor any person acting on behalf of the United States Government assumes any liability resulting from the use of the information contained in this document, or warrants that such use will be free from privately owned rights.



Airport Remote Tower Sensor Systems

Better weather information will be available for guiding approaches and landings.

Ames Research Center, Moffett Field, California

Networks of video cameras, meteorological sensors, and ancillary electronic equipment are under development in collaboration among NASA Ames Research Center, the Federal Aviation Administration (FAA), and the National Oceanic Atmospheric Administration (NOAA). These networks are to be established at and near airports to provide real-time information on local weather conditions that affect aircraft approaches and landings.

The prototype network is an airport approach-zone camera system (AAZCS), which has been deployed at San Francisco International Airport (SFO) and San Carlos Airport (SQL). The AAZCS includes remotely controlled color video cameras located on top of SFO and SQL air-traffic control towers. The

cameras are controlled by the NOAA Center Weather Service Unit located at the Oakland Air Route Traffic Control Center and are accessible via a secure Web site. The AAZCS cameras can be zoomed and can be panned and tilted to cover a field of view 220° wide. The NOAA observer can see the sky condition as it is changing, thereby making possible a real-time evaluation of the conditions along the approach zones of SFO and SQL.

The next-generation network, denoted a remote tower sensor system (RTSS), will soon be deployed at the Half Moon Bay Airport and a version of it will eventually be deployed at Los Angeles International Airport. In addition to remote control of video cameras via secure Web links, the RTSS offers real-time weather observations, remote sens-

ing, portability, and a capability for deployment at remote and uninhabited sites. The RTSS can be used at airports that lack control towers, as well as at major airport hubs, to provide synthetic augmentation of vision for both local and remote operations under what would otherwise be conditions of low or even zero visibility.

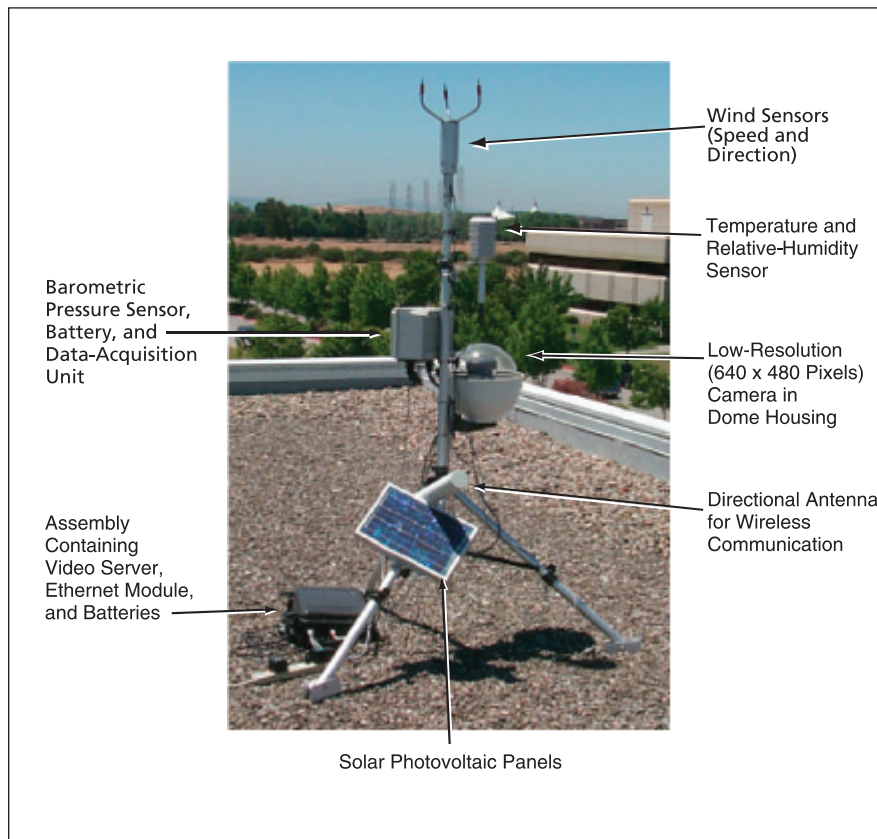
A prototype of a portable RTSS unit (see figure) includes a tripod, on which are mounted the following subsystems:

- A low-resolution pan/tilt/zoom color video camera in a dome housing;
- Ultrasonic sensors for measuring wind velocity;
- Temperature and relative-humidity sensors;
- A barometric pressure sensor;
- A data-acquisition (data-logging) subsystem for collecting sensor data;
- An embedded Web video-image-data server computer;
- A wireless Ethernet module;
- A battery power supply;
- Solar photovoltaic panels to charge the battery; and
- A directional antenna for wireless communication.

In addition to portable units like this one, the RTSS will include a high-resolution camera mounted on a pre-existing airport tower.

It is envisioned that future RTSSs will be parts of dynamic virtual tower systems, which will be air-traffic-control systems that will serve airports that lack control towers. In a virtual tower system, the information collected from a suite of RTSS units would be sent to a facility, located elsewhere than at an affected airport, where a team of air-traffic controllers could utilize the information in performing real-time tower operations. It is further envisioned that real-time integration of data among pilots, aircraft, and virtual tower stations will become feasible.

Yet another development is that of a real-time, automated visibility-image-management system that uses RTSSs to track changing airport and terminal



A **Prototype RTSS Portable Unit** includes sensor, power, and communication subsystems mounted on a 9-ft (=2.7-m) tripod.

conditions. More specifically, this system processes RTSS image data, by use of advanced algorithms, to predict trends in visibility. The image data are acquired, stored, and processed at 15-minute intervals. The processing of the data yields 15-minute updates of a

visibility-versus-time plot, on which visibility is quantified on a suggested scale of 0 to 1.

This work was done by David A. Maluf, Yuri Gawdiak, Christopher Leidichj, and Richard Papasin of Ames Research Center and Peter B. Tran and Kevin Bass of QSS

Group, Inc. Further information is contained in a TSP (see page 1).

Inquiries concerning rights for the commercial use of this invention should be addressed to the Ames Technology Partnerships Division at (650) 604-2954. Refer to ARC-15029-1.

Implantable Wireless MEMS Sensors for Medical Uses

Integrated Sensing Systems, Inc., Ypsilanti, Michigan

Sensors designed and fabricated according to the principles of microelectromechanical systems (MEMS) are being developed for several medical applications in outer space and on Earth. The designs of these sensors are based on a core design family of pressure sensors, small enough to fit into the eye of a needle, that are fabricated by a “dissolved wafer” process. The sensors are expected to be implantable, batteryless, and wireless. They would be both powered and interrogated by hand-held radio trans-

ceivers from distances up to about 6 in. (about 15 cm). One type of sensor would be used to measure blood pressure, particularly for congestive heart failure. Another type would be used to monitor fluids in patients who have hydrocephalus (high brain pressure). Still other types would be used to detect errors in delivery of drugs and to help patients having congestive heart failure.

This work was directed by Alexander Chimbayo of Integrated Sensing Systems, Inc. under a NASA Small Business Inno-

vation Research (SBIR) contract monitored by Langley Research Center. For further information, contact:

Dr. Alexander Chimbayo

Integrated Sensing Systems, Inc.

391 Airport Industrial Drive

Ypsilanti, MI 48198

Phone No.: (734) 547-9896 Ext. 116

E-mail: alec@mems-issys.com

Refer to SBIR-0010, volume and number of this NASA Tech Briefs issue, and the page number.

Embedded Sensors for Measuring Surface Regression

Electrical-resistance measurements are translated into real-time material thickness and surface regression data for hybrid fuels, solid propellants, and ablative materials.

Stennis Space Center, Mississippi

The development and evaluation of new hybrid and solid rocket motors requires accurate characterization of the propellant surface regression as a function of key operational parameters. These characteristics establish the propellant flow rate and are prime design drivers affecting the propulsion system geometry, size, and overall performance. There is a similar need for the development of advanced ablative materials, and the use of conventional ablatives exposed to new operational environments. The Miniature Surface Regression Sensor (MSRS) was developed to serve these applications. It is designed to be cast or embedded in the material of interest and regresses along with it. During this process, the resistance of the sensor is related to its instantaneous length, allowing the real-time thickness of the host material to be established. The time derivative of this data reveals the instantaneous surface regression rate.

The MSRS could also be adapted to perform similar measurements for a variety of other host materials when it is desired to monitor thicknesses and/or regression rate for purposes of safety, operational control, or research. For example, the sensor could be used to monitor the thicknesses of brake linings or racecar tires and indicate when they need to be replaced. At the time of this reporting, over 200 of these sensors have been installed into a variety of host materials.

An MSRS can be made in either of two configurations, denoted “ladder” and “continuous” (see Figure 1). A ladder MSRS includes two highly electrically conductive legs, across which narrow strips of electrically resistive material are placed at small increments of length. These strips resemble the rungs of a ladder and are electrically equivalent to many tiny resistors connected in parallel. A substrate material provides structural support for the legs and rungs. The instantaneous sensor

resistance is read by an external signal conditioner via wires attached to the conductive legs on the non-eroding end of the sensor. The sensor signal can be transmitted from inside a high-pressure chamber to the ambient environment, using commercially available feedthrough connectors. Miniaturized internal recorders or wireless data transmission could also potentially be employed to eliminate the need for producing penetrations in the chamber case.

The rungs are designed so that as each successive rung is eroded away, the resistance changes by an amount that yields a readily measurable signal larger than the background noise. (In addition, signal-conditioning techniques are used in processing the resistance readings to mitigate the effect of noise.) Hence, each discrete change of resistance serves to indicate the arrival of the regressing host material front at the known depth of the affected resistor rung. The average rate of regression between two adjacent resis-

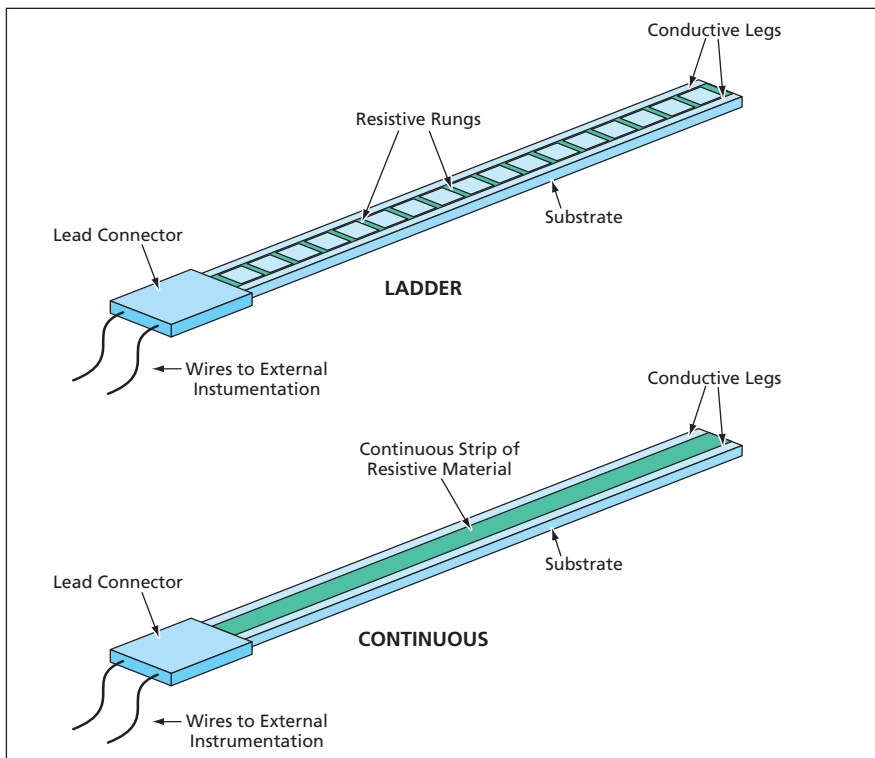


Figure 1. The **Two Baseline MSRS Configurations** offer different features. The ladder configuration gives readings in precise increments of material thickness, while the continuous configuration gives a constant indication of material thickness.

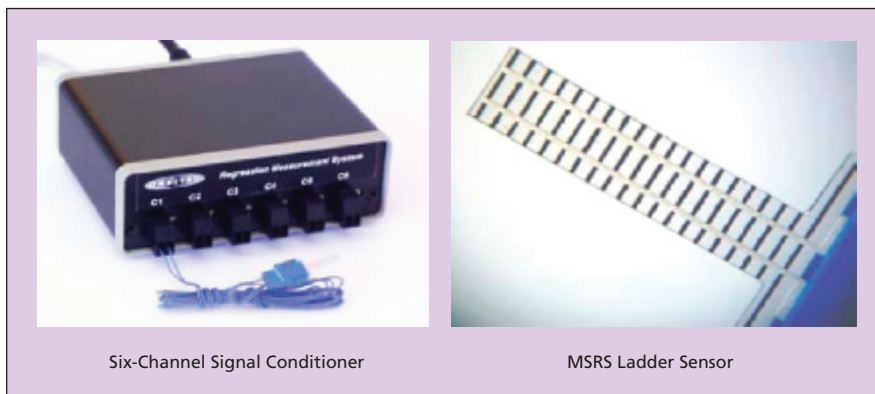


Figure 2. A **Ground-Based MSRS Sensor Package** has been developed that features small size and low mass. Future generations of the MSRS technology could be used to transmit real-time regression rate and material thickness data from a vehicle in flight.

tors can be calculated simply as the distance between the resistors divided by the time interval between their resistance jumps. Advanced data reduction techniques have also been developed to establish the instantaneous surface position and regression rate when the regressing front is between rungs.

A continuous MSRS is so named because instead of discrete rungs, there is one continuous strip of resistive material across the legs. Assuming that this strip has spatially uniform thickness and resistivity and that the electrical resistance of the legs is much less than that of the strip, the electrical resistance of this MSRS is inversely proportional to the remaining length of the sensor and, hence, to the remaining thickness of the host material in which it is embedded.

A ground-based sensor package has been developed (see Figure 2). Due to its small size and low mass potential, future generations of the MSRS technology could be applied to flight applications. One eventual goal is to provide the capability to record and transmit real-time regression data from a vehicle in flight. In this capacity, the sensor could serve a dual-use role by providing engineering data under actual operating conditions, as well as health monitoring of the host material.

This work was done by Daniel J. Gramer, Thomas J. Taagen, and Anton G. Vermaak of Orbital Technologies Corp. for Stennis Space Center.

In accordance with Public Law 96-517, the contractor has elected to retain title to this invention. Inquiries concerning rights for its commercial use should be addressed to:

*Orbital Technologies Corp. (ORBITEC)
1212 Fourier Dr.
Madison, WI 53717
Phone No.: (608) 827-5000*

Refer to SSC-00140, volume and number of this NASA Tech Briefs issue, and the page number.

Coordinating an Autonomous Earth-Observing Sensorweb

NASA's Jet Propulsion Laboratory, Pasadena, California

A system of software has been developed to coordinate the operation of an autonomous Earth-observing sensorweb. Sensorwebs are collections of sensor units scattered over large regions to gather data on spatial and temporal patterns of physical, chemical, or biological phenomena in those regions. Each sensor unit is a node in a data-

gathering/data-communication network that spans a region of interest. In this case, the region is the entire Earth, and the sensorweb includes multiple terrestrial and spaceborne sensor units. In addition to acquiring data for scientific study, the sensorweb is required to give timely notice of volcanic eruptions, floods, and other hazardous natural

events. In keeping with the inherently modular nature of the sensory, communication, and data-processing hardware, the software features a flexible, modular architecture that facilitates expansion of the network, customization of conditions that trigger alarms of hazardous natural events, and customization of responses to alarms. The soft-

ware facilitates access to multiple sources of data on an event of scientific interest, enables coordinated use of multiple sensors in rapid reaction to detection of an event, and facilitates the tracking of spacecraft operations, including tracking of the acquisition, pro-

cessing, and downlinking of requested data.

This program was written by Robert Sherwood, Benjamin Cichy, Daniel Tran, Steve Chien, Gregg Rabideau, Ashley Davies, Rebecca Castaño, Stuart Frye, Dan Mandl, Seth Shulman, and Sandy Grosvenor of Cal-

tech for NASA's Jet Propulsion Laboratory. Further information is contained in a TSP (see page 1).

This software is available for commercial licensing. Please contact Karina Edmonds of the California Institute of Technology at (626) 395-2322. Refer to NPO-42523.

Range-Measuring Video Sensors

Distances would be measured by three-dimensional triangulation.

Marshall Space Flight Center, Alabama

Optoelectronic sensors of a proposed type would perform the functions of both electronic cameras and triangulation-type laser range finders. That is to say, these sensors would both (1) generate ordinary video or snapshot digital

images and (2) measure the distances to selected spots in the images. These sensors would be well suited to use on robots that are required to measure distances to targets in their work spaces. In addition, these sensors could be used for

all the purposes for which electronic cameras have been used heretofore.

The simplest sensor of this type, illustrated schematically in the upper part of the figure, would include a laser, an electronic camera (either video or snapshot), a frame-grabber/image-capturing circuit, an image-data-storage memory circuit, and an image-data processor. There would be no moving parts. The laser would be positioned at a lateral distance d to one side of the camera and would be aimed parallel to the optical axis of the camera. When the range of a target in the field of view of the camera was required, the laser would be turned on and an image of the target would be stored and preprocessed to locate the angle (α) between the optical axis and the line of sight to the centroid of the laser spot. Then the range, r (more precisely, the length of the optical-axis component of the range vector) of the laser-illuminated spot on the target would be given by

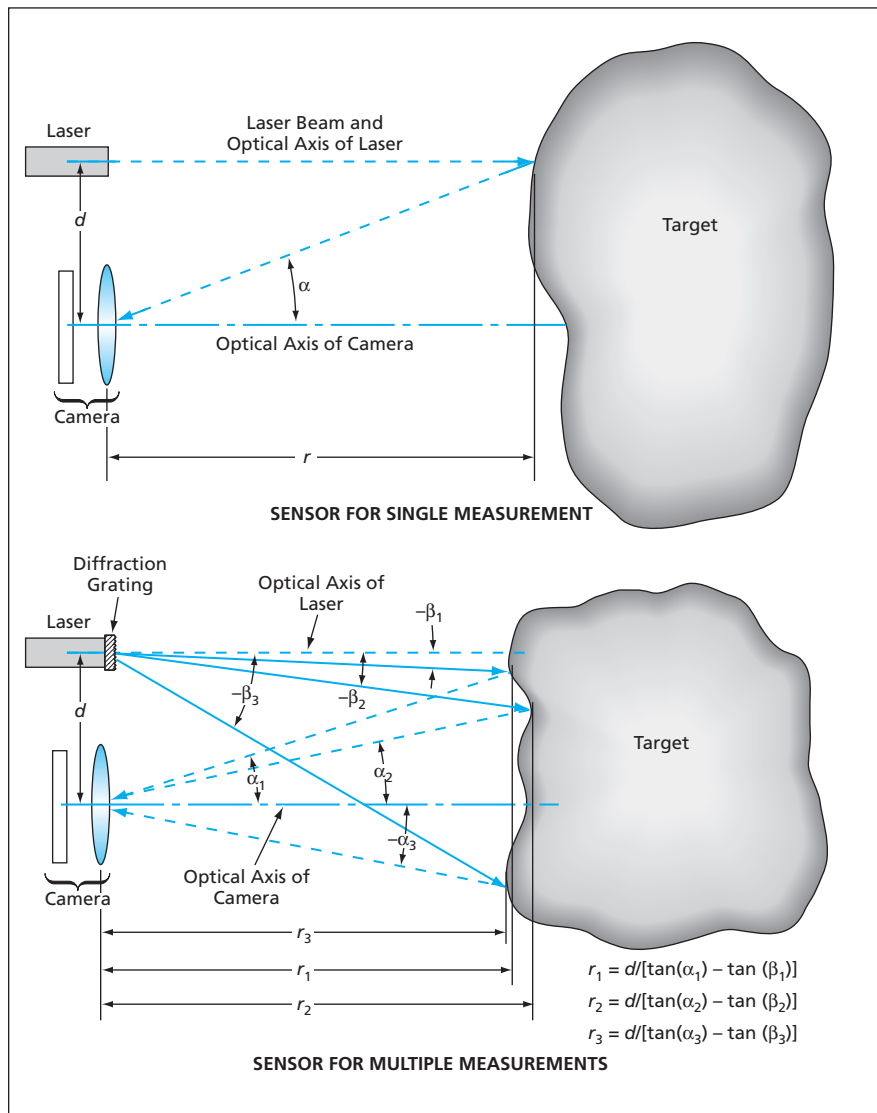
$$r = d / \tan(\alpha).$$

The lower part of the figure depicts a more complex sensor that could measure the ranges of multiple targets or multiple spots on the same target. The basic optical arrangement would be as described above, except that a diffraction grating would split the laser beam into multiple beams, each at a different angle in the plane defined by the camera and laser optical axes. In this case, the range of the spot illuminated by the i th laser beam would be given by

$$r_i = d / [\tan(\alpha_i) - \tan(\beta_i)],$$

where β_i is the angle of the i th beam and all angles are measured as positive above or negative below the horizontal optical axes in the figure.

This work was done by Richard T. Howard, Jeri M. Briscoe, Eric L. Corder, and David Broderick of Marshall Space Flight Center. Further information is contained in a TSP (see page 1). MFS-31891-1



These Two Sensors would utilize triangulation to measure ranges. The simpler sensor is shown at the top, mainly to help explain the basic principle of operation. The more complex sensor shown at the bottom would likely be preferable in practice.

Stability Enhancement of Polymeric Sensing Films Using Fillers

Enhanced stability of polymer sensing films is achieved by adding colloidal fillers.

NASA's Jet Propulsion Laboratory, Pasadena, California

Experiments have shown the stability enhancement of polymeric sensing films on mixing the polymer with colloidal filler particles (submicron-sized) of carbon black, silver, titanium dioxide, and fumed silicon dioxide. The polymer films are candidates for potential use as sensing media in micro/nano chemical sensor devices. The need for stability enhancement of polymer sensing films arises because

such films have been found to exhibit unpredictable changes in sensing activity over time, which could result in a possible failure of the sensor device.

The changes in the physical properties of a polymer sensing film caused by the sorption of a target molecule can be measured by any of several established transduction techniques: electrochemical, optical, calorimetric, or piezoelec-

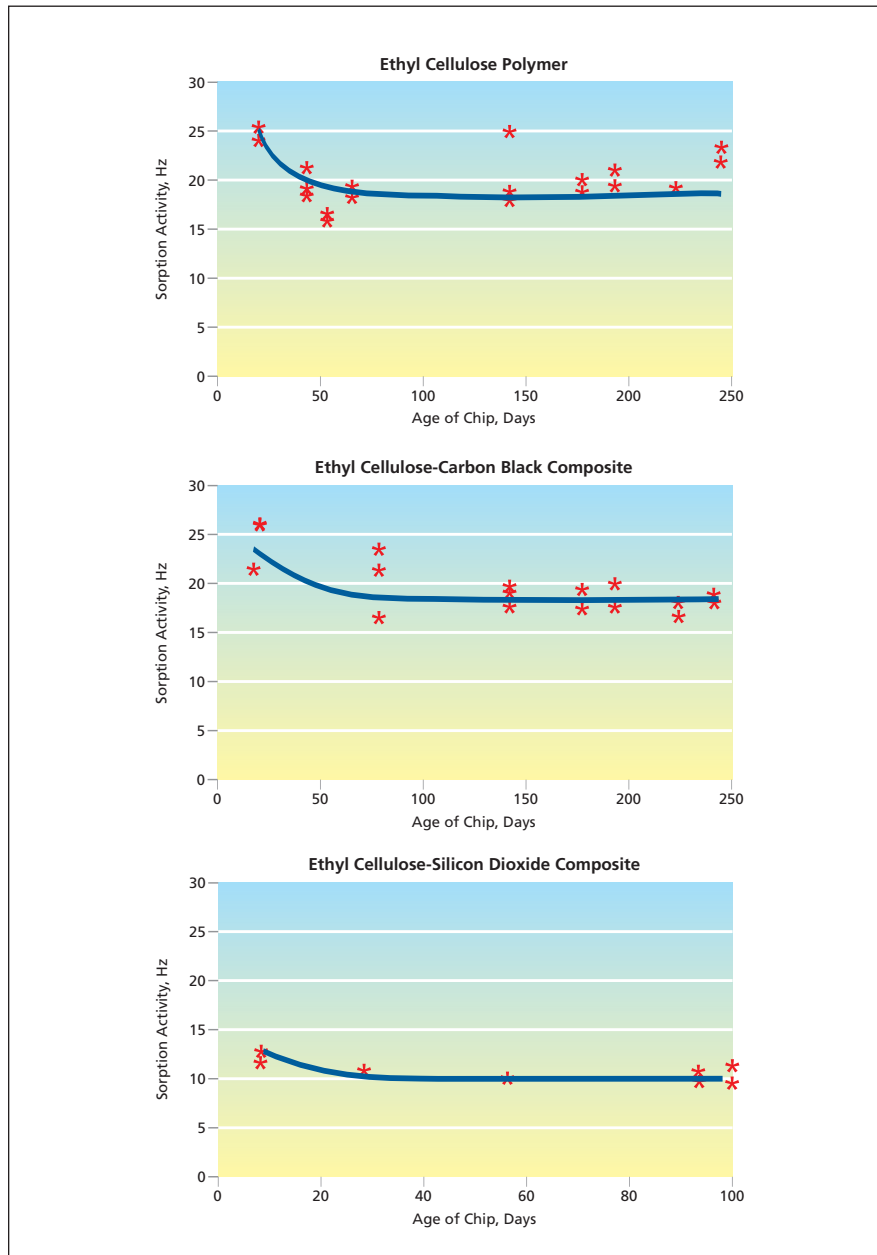
tric, for example. The transduction technique used in the current polymer stability experiments is based on piezoelectric principles using a quartz-crystal microbalance (QCM). The surface of the QCM is coated with the polymer, and the mass uptake by the polymer film causes a change in the oscillation frequency of the quartz crystal.

The polymer used for the current study is ethyl cellulose. The polymer/polymer composite solutions were prepared in 1,3 dioxolane solvent. The filler concentration was fixed at 10 weight percent for the composites. The polymer or polymer composite solutions were cast on the quartz crystal having a fundamental frequency of about 6 MHz. The coated crystal was subjected to a multistage drying process to remove all measurable traces of the solvent.

In each experiment, the frequency of oscillation was measured while the QCM was exposed to clean, dry, flowing air for about 30 minutes, then to air containing a known concentration of isopropanol for about 30 minutes, then again to clean dry air for about 30 minutes, and so forth. This cycle of measurements for varying isopropanol concentrations was repeated at intervals for several months.

The figure depicts some of the sensing film stability results for ethyl cellulose polymer, ethyl cellulose-carbon black, and ethyl cellulose-silicon dioxide composite systems. An ethyl cellulose film exhibited a marked decline in response in the first few months of study and settled to a steady average response after about four months. However, response varied widely around the average response for ethyl cellulose film. In contrast, ethyl cellulose-carbon black and ethyl cellulose-silicon dioxide composites also declined in the early months, but showed more repeatable sensing film activity after the initial decline. Similar trends were observed in experiments for ethyl cellulose-titanium dioxide and ethyl cellulose-silver composites.

This work was done by Brian Lin, Abhijit Shevade, Margaret Amy Ryan, Adam Kisor, Shiao-Pin Yen, Kenneth Manatt, Margie Homer, and Jean-Pierre Fleurial of Caltech for NASA's Jet Propulsion Laboratory. Further information is contained in a TSP (see page 1). NPO-40518



Graphs Show Sensing Stabilities of ethyl cellulose polymer and ethyl cellulose-composite sensing films to the detection of 600 ppm of isopropanol. As compared to the stability of ethyl cellulose polymer, the ethyl cellulose-carbon composite and ethyl cellulose-silicon dioxide composite show greater stability with time. The lines drawn are to guide the eye.

⊕ Sensors for Using Times of Flight To Measure Flow Velocities

No calibrations are needed to use these thin-film sensors.

John H. Glenn Research Center, Cleveland, Ohio

Thin-film sensors for measuring flow velocities in terms of times of flight are undergoing development. These sensors are very small and can be mounted flush with surfaces of airfoils, ducts, and other objects along which one might need to measure flows. Alternatively or in addition, these sensors can be mounted on small struts protruding from such surfaces for acquiring velocity measurements at various distances from the surfaces for the purpose of obtaining boundary-layer flow-velocity profiles.

These sensors are related to, but not the same as, hot-wire anemometers. Each sensor includes a thin-film, electrically conductive loop, along which an electric current is made to flow to heat the loop to a temperature above that of the surrounding fluid. Instanta-

neous voltage fluctuations in segments of the loop are measured by means of electrical taps placed at intervals along the loop. These voltage fluctuations are caused by local fluctuations in electrical resistance that are, in turn, caused by local temperature fluctuations that are, in turn, caused by fluctuations in flow-induced cooling and, hence, in flow velocity.

The differential voltage as a function of time, measured at each pair of taps, is subjected to cross-correlation processing with the corresponding quantities measured at other pairs of taps at different locations on the loop. The cross-correlations yield the times taken by elements of fluid to travel between the pairs of taps. Then the component of velocity along the line between any

two pairs of taps is calculated simply as the distance between the pairs of taps divided by the travel time. Unlike in the case of hot-wire anemometers, there is no need to obtain calibration data on voltage fluctuations versus velocity fluctuations because, at least in principle, the correlation times are independent of the calibration data.

This work was done by Gutave Fralick, John D. Wrbanek, and Danny Hwang of Glenn Research Center and James Turso of QSS Inc. Further information is contained in a TSP (see page 1).

Inquiries concerning rights for the commercial use of this invention should be addressed to NASA Glenn Research Center, Innovative Partnerships Office, Attn: Steve Fedor, Mail Stop 4-8, 21000 Brookpark Road, Cleveland, Ohio 44135. Refer to LEW-17944-1.



Receiver Would Control Phasing of a Phased-Array Antenna

Peaks and nulls would be aimed to optimize reception.

NASA's Jet Propulsion Laboratory, Pasadena, California

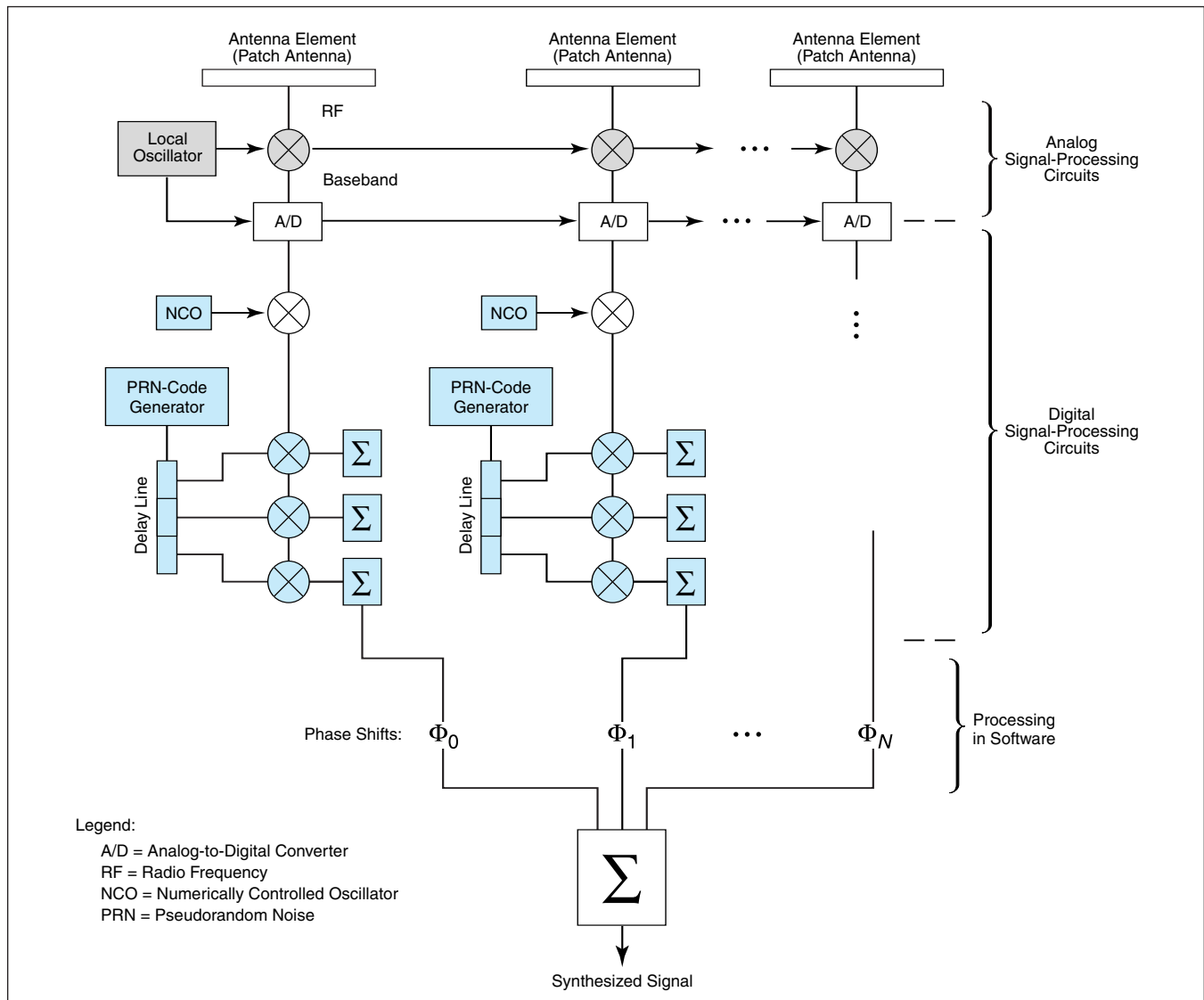
In a proposed digital signal-processing technique, a radio receiver would control the phasing of a phased-array antenna to aim the peaks of the antenna radiation pattern toward desired signal sources while aiming the nulls of the pattern toward interfering signal sources. The technique was conceived for use in a Global Positioning System (GPS) receiver, for which the desired signal sources would be GPS satellites and typi-

cal interference sources would be terrestrial objects that cause multipath propagation. The technique could also be used to optimize reception in spread-spectrum cellular-telephone and military communication systems.

During reception of radio signals in a conventional phased-array antenna system, received signals at their original carrier frequencies are phase-shifted, then combined by analog circuitry. The

combination signal is then subjected to downconversion and demodulation.

In a system according to the proposed technique (see figure), the signal received by each antenna would be subjected to downconversion, spread-spectrum demodulation, and correlation; this processing would be performed separately from, and simultaneously with, similar processing of signals received by the other antenna elements. Following ana-



Baseband Signals Would Be Digitized and processed in parallel. Phase shifts could be added in software to aim the peaks and nulls of the antenna radiation pattern; the effect would be equivalent to that of beam steering by phase shifting in hardware.

log downconversion to baseband, the signals would be digitized, and all subsequent processing would be digital.

In the digital process, residual carriers would be removed and each signal would be correlated with a locally generated model pseudorandom-noise code, all following normal GPS procedure. As part of this procedure, accumulated values would be added in software and the resulting signals would be phase-shifted in software by the amounts necessary to synthesize the desired antenna directional gain pattern of peaks and nulls.

The principal advantage of this technique over the conventional radio-frequency-combining technique is that the parallel digital baseband processing of the signals from the various antenna elements would be a relatively inexpensive and flexible means for exploiting the inherent multiple-peak/multiple-null aiming capability of a phased-array antenna. In the original intended GPS application, the peaks and nulls could be directed independently for each GPS signal being tracked by the GPS receiver. The technique could also be applied to other

code-division multiple-access communication systems.

This work was done by Charles E. Dunn and Lawrence E. Young of Caltech for NASA's Jet Propulsion Laboratory. Further information is contained in a TSP (see page 1).

This invention is owned by NASA, and a patent application has been filed. Inquiries concerning nonexclusive or exclusive license for its commercial development should be addressed to the Patent Counsel, NASA Management Office-JPL, (818) 354-7770. Refer to NPO-20031.

Modern Design of Resonant Edge-Slot Array Antennas

Better antennas can be designed at lower cost.

Goddard Flight Space Center, Greenbelt, Maryland

Resonant edge-slot (slotted-waveguide) array antennas can now be designed very accurately following a modern computational approach like that followed for some other microwave components. This modern approach makes it possible to design superior antennas at lower cost than was previously possible.

Heretofore, the physical and engineering knowledge of resonant edge-slot array antennas had remained immature since they were introduced during World War II. This is because despite their mechanical simplicity, high reliability, and potential for operation with high efficiency, the electromagnetic behavior of resonant edge-slot antennas is very complex. Because engineering design formulas and curves for such antennas are not available in the open literature, designers have been forced to implement iterative processes of fabricating and testing multiple prototypes to derive design databases, each unique for a specific combination of operating frequency and set of waveguide tube dimensions. The expensive, time-consuming nature of these processes has inhibited the use of resonant edge-slot antennas. The present modern approach reduces costs by making it unnecessary to build and test multiple prototypes. As an additional benefit, this approach affords a capability to design an array of slots having different dimensions to taper the antenna illumination to reduce the amplitudes of unwanted side lobes.

The heart of the modern approach is the use of the latest commercially available microwave-design software, which implements finite-element models of electromagnetic fields in and around waveguides, antenna elements, and sim-

ilar components. Instead of building and testing prototypes, one builds a database and constructs design curves from the results of computational simulations for sets of design parameters.

The figure shows a resonant edge-



This **Resonant Edge-Slot Antenna** with tapered illumination was designed on the basis of computational simulations, instead of following the traditional approach of iterative fabrication and testing of prototypes.

slot antenna designed following this approach. Intended for use as part of a radiometer operating at a frequency of 10.7 GHz, this antenna was fabricated from dimensions defined exclu-

sively by results of computational simulations. The final design was found to be well optimized and to yield performance exceeding that initially required.

*This work was done by R. B. Gosselin of Goddard Space Flight Center. Further information is contained in a TSP (see page 1).
GSC-14747-1*

Carbon-Nanotube Schottky Diodes

These devices can outperform conventional Schottky diodes at submillimeter wavelengths.

NASA's Jet Propulsion Laboratory, Pasadena, California

Schottky diodes based on semiconducting single-walled carbon nanotubes are being developed as essential components of the next generation of submillimeter-wave sensors and sources. Initial performance predictions have shown that the performance characteristics of these devices can exceed those of the state-of-the-art solid-state Schottky diodes that have been the components of choice for room-temperature submillimeter-wave sensors for more than 50 years.

For state-of-the-art Schottky diodes used as detectors at frequencies above a few hundred gigahertz, the inherent parasitic capacitances associated with their semiconductor junction areas and the resistances associated with low electron mobilities limit achievable sensitivity. The performance of such a detector falls off approximately exponentially with frequency above 500 GHz. Moreover, when used as frequency multipliers for generating signals, state-of-the-art solid-state Schottky diodes exhibit extremely low efficiencies, generally putting out only microwatts of power at fre-

quencies up to 1.5 THz.

The shortcomings of the state-of-the-art solid-state Schottky diodes can be overcome by exploiting the unique electronic properties of semiconducting carbon nanotubes. A single-walled carbon nanotube can be metallic or semiconducting, depending on its chirality, and exhibits high electron mobility (recently reported to be $\approx 2 \times 10^5$ cm²/V-s) and low parasitic capacitance. Because of the narrowness of nanotubes, Schottky diodes based on carbon nanotubes have ultra-small junction areas (of the order of a few square nanometers) and consequent junction capacitances of the order of 10^{-18} F, which translates to cut-off frequency >5 THz. Because the turn-on power levels of these devices are very low (of the order of nanowatts), the input power levels needed for pumping local oscillators containing these devices should be lower than those needed for local oscillators containing state-of-the-art solid-state Schottky diodes.

In terms that are necessarily simplified for the sake of brevity, a carbon-nanotube-based Schottky diode is fabricated

in a process that features evaporative deposition of dissimilar metal contacts onto opposite ends of a semiconducting single-walled carbon nanotube. One of the metals (platinum in initial experiments) is chosen to have a work function greater than that of the carbon nanotube, so as to form an ohmic contact. The other metal (titanium in initial experiments) is chosen to have a work function less than that of the carbon nanotube, so as to form a Schottky contact. These metals are then covered with outer layers of gold. The figure shows the rectifying behavior of four experimental devices fabricated in such a process.

To reduce the effective series resistance, it is preferable to fabricate such a device in the form of a set of multiple parallel single-wall carbon nanotubes, grown on the same substrate, bridging the gap between the higher- and the lower-work-function metal contact. Usually, in such a case, some of the carbon nanotubes turn out to be metallic and, hence, must be removed to obtain the desired rectifying behavior. Removal can be effected by a previously published procedure in which the semiconducting nanotubes are gated off and the metallic ones are selectively burned out.

This work was done by Harish Manohara, Eric Wong, Erich Schlecht, Brian Hunt, and Peter Siegel of Caltech for NASA's Jet Propulsion Laboratory. Further information is contained in a TSP (see page 1).

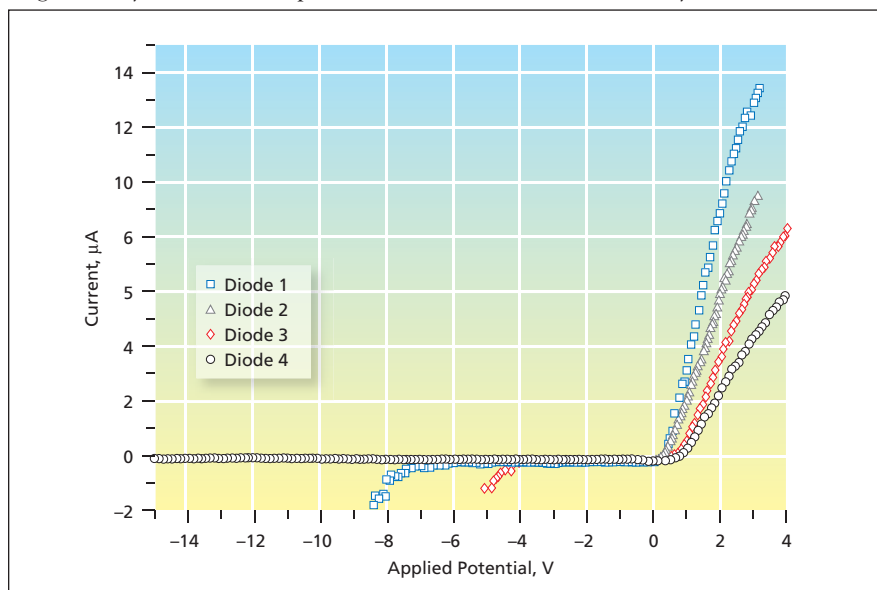
In accordance with Public Law 96-517, the contractor has elected to retain title to this invention. Inquiries concerning rights for its commercial use should be addressed to:

*Innovative Technology Assets Management
JPL*

*Mail Stop 202-233
4800 Oak Grove Drive
Pasadena, CA 91109-8099
(818) 354-2240*

E-mail: iaoffice@jpl.nasa.gov

Refer to NPO-42067, volume and number of this NASA Tech Briefs issue, and the page number.



Rectifying Behavior is apparent in the DC current-versus-voltage characteristics of four experimental carbon-nanotube-based Schottky diodes that were fabricated on the same substrate.

Simplified Optics and Controls for Laser Communications

NASA's Jet Propulsion Laboratory, Pasadena, California

A document discusses an architecture of a spaceborne laser communication system that provides for a simplified control subsystem that stabilizes the line of sight in a desired direction. Heretofore, a typical design for a spaceborne laser communication system has called for a high-bandwidth control loop, a steering mirror and associated optics, and a fast steering-mirror actuator to stabilize the line of sight in the presence of vibrations. In the present architecture, the need for this fast

steering-mirror subsystem is eliminated by mounting the laser-communication optics on a disturbance-free platform (DFP) that suppresses coupling of vibrations to the optics by ≥ 60 dB. Taking advantage of microgravity, in the DFP, the optical assembly is free-flying relative to the rest of the spacecraft, and a low-spring-constant pointing control subsystem exerts small forces to regulate the position and orientation of the optics via voice coils. All steering is effected via the DFP, which can

be controlled in all six degrees of freedom relative to the spacecraft. A second control loop, closed around a position sensor and the spacecraft attitude-control system, moves the spacecraft as needed to prevent mechanical contact with the optical assembly.

This work was done by Chien-Chung Chen and Hamid Hemmati of Caltech for NASA's Jet Propulsion Laboratory. Further information is contained in a TSP (see page 1). NPO-42693

Coherent Detection of High-Rate Optical PPM Signals

Quantum-limited performance is achievable.

NASA's Jet Propulsion Laboratory, Pasadena, California

A method of coherent detection of high-rate pulse-position modulation (PPM) on a received laser beam has been conceived as a means of reducing the deleterious effects of noise and atmospheric turbulence in free-space optical communication using focal-plane detector array technologies. In comparison with a receiver based on direct detection of the intensity modulation of a PPM signal, a receiver based on the present method of coherent detection performs well at much higher background levels.

In principle, the coherent-detection receiver can exhibit quantum-limited performance despite atmospheric tur-

bulence. The key components of such a receiver include standard receiver optics, a laser that serves as a local oscillator, a focal-plane array of photodetectors, and a signal-processing and data-acquisition assembly needed to sample the focal-plane fields and reconstruct the pulsed signal prior to detection. The received PPM-modulated laser beam and the local-oscillator beam are focused onto the photodetector array, where they are mixed in the detection process. The two lasers are of the same or nearly the same frequency. If the two lasers are of different frequencies, then

the coherent detection process is characterized as heterodyne and, using traditional heterodyne-detection terminology, the difference between the two laser frequencies is denoted the intermediate frequency (IF). If the two laser beams are of the same frequency and remain aligned in phase, then the coherent detection process is characterized as homodyne (essentially, heterodyne detection at zero IF).

As a result of the inherent squaring operation of each photodetector, the output current includes an IF component that contains the signal modulation. The amplitude of the IF component is proportional to the product of the local-oscillator signal amplitude and the PPM signal amplitude. Hence, by using a sufficiently strong local-oscillator signal, one can make the PPM-modulated IF signal strong enough to overcome thermal noise in the receiver circuits: this is what makes it possible to achieve near-quantum-limited detection in the presence of strong background.

Following quantum-limited coherent detection, the outputs of the individual photodetectors are automatically aligned in phase by use of one or more adaptive array compensation algorithms [e.g., the least-mean-square (LMS) algorithm]. Then the outputs are combined and the resulting signal is processed to extract the high-rate information, as though the PPM signal were received by a single photodetector.

In a continuing series of experiments

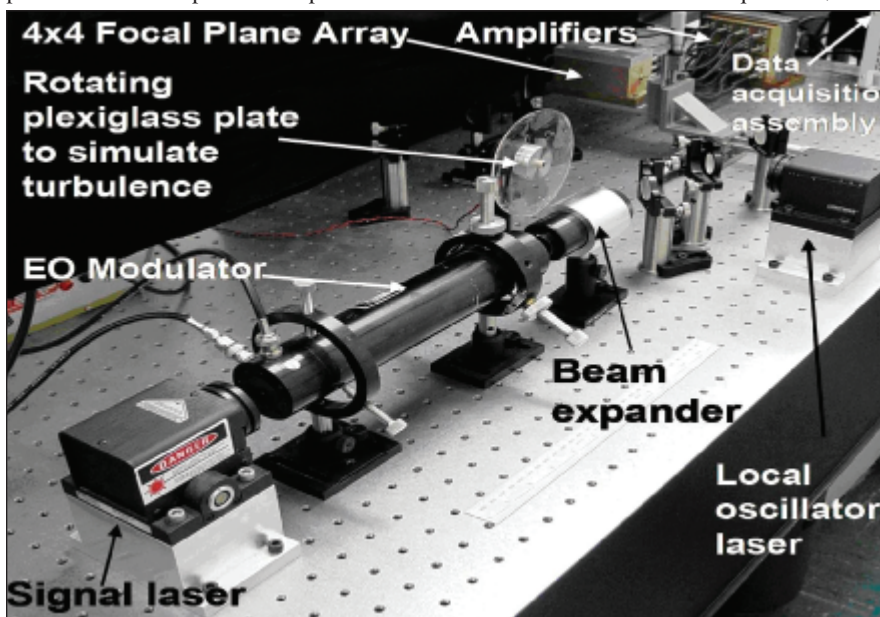


Figure 1. A Coherent Optical Receiver as it is set up for experiments at NASA's Jet Propulsion Laboratory.

to test this method (see Fig. 1), the local oscillator has a wavelength of 1,064 nm, and another laser is used as a signal transmitter at a slightly different wavelength to establish an IF of about 6 MHz. There are 16 photodetectors in a 4x4 focal-plane array; the detector outputs are digitized at a sampling rate of 25 MHz, and the signals in digital form are combined by use of the LMS algorithm. Convergence of the adaptive combining algorithm in the presence of

simulated atmospheric turbulence for optical PPM signals has already been demonstrated in the laboratory; the combined output is shown in Fig. 2(a), and Fig. 2(b) shows the behavior of the phase of the combining weights as a function of time (or samples). We observe that the phase of the weights has a sawtooth shape due to the continuously changing phase in the down-converted output, which is not exactly at zero frequency.

Detailed performance analysis of this coherent free-space optical communication system in the presence of simulated atmospheric turbulence is currently under way.

*This work was done by Victor Vilnrotter and Michela Muñoz Fernández of Caltech for NASA's Jet Propulsion Laboratory. Further information is contained in a TSP (see page 1).
NPO-40974*

Multichannel Phase and Power Detector

Purposes served by this system include beam steering and power combining.

NASA's Jet Propulsion Laboratory, Pasadena, California

An electronic signal-processing system determines the phases of input signals arriving in multiple channels, relative to the phase of a reference signal with which the input signals are known to be coherent in both phase and frequency. The system also gives an estimate of the power levels of the input signals. A prototype of the system has four input channels that handle signals at a frequency of ≈ 9.5 MHz, but the basic principles of design and operation are extensible to other signal frequencies and greater numbers of channels.

The prototype system consists mostly of three parts:

- An analog-to-digital-converter (ADC) board, which coherently digitizes the input signals in synchronism with the reference signal and performs some simple processing;
- A digital signal processor (DSP) in the form of a field-programmable gate

array (FPGA) board, which performs most of the phase- and power-measurement computations on the digital samples generated by the ADC board; and

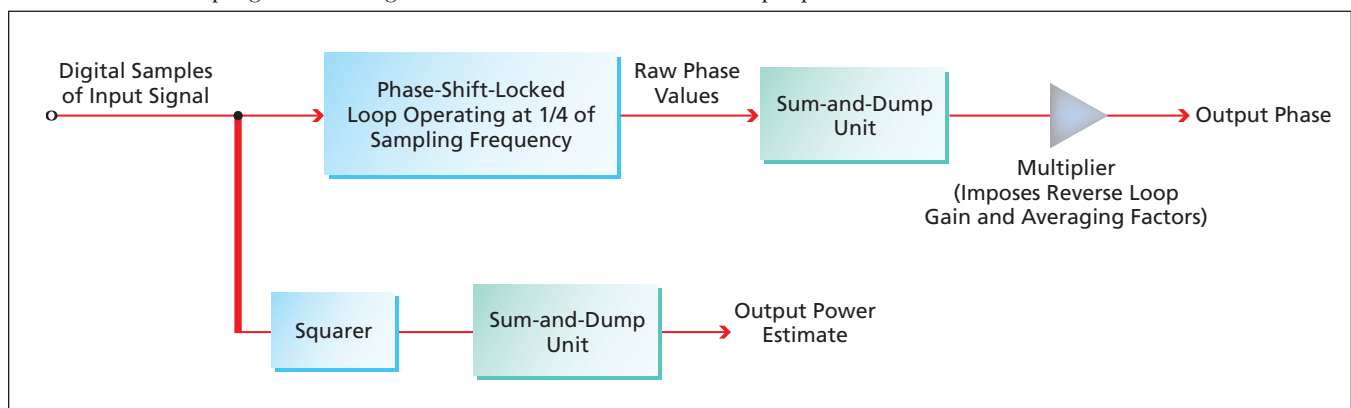
- A carrier board, which allows a personal computer to retrieve the phase and power data.

The DSP contains four independent phase-only tracking loops, each of which tracks the phase of one of the pre-processed input signals relative to that of the reference signal (see figure). The phase values computed by these loops are averaged over intervals, the length of which is chosen to obtain output from the DSP at a desired rate. In addition, a simple sum of squares is computed for each channel as an estimate of the power of the signal in that channel.

The relative phases and the power level estimates computed by the DSP could be used for diverse purposes in

different settings. For example, if the input signals come from different elements of a phased-array antenna, the phases could be used as indications of the direction of arrival of a received signal and/or as feedback for electronic or mechanical beam steering. The power levels could be used as feedback for automatic gain control in preprocessing of incoming signals. For another example, the system could be used to measure the phases and power levels of outputs of multiple power amplifiers to enable adjustment of the amplifiers for optimal power combining.

*This work was done by Samuel Li, James Lux, Robert McMaster, and Amy Boas of Caltech for NASA's Jet Propulsion Laboratory. Further information is contained in a TSP (see page 1).
NPO-42697*



A Functional Block Diagram of the DSP shows one channel. The other channels are identical.



Using Satellite Data in Weather Forecasting: I

The GOES Product Generation System (GPGS) is a set of computer codes and scripts that enable the assimilation of real-time Geostationary Operational Environmental Satellite (GOES) data into regional-weather-forecasting mathematical models. The GPGS can be used to derive such geophysical parameters as land surface temperature, the amount of precipitable water, the degree of cloud cover, the surface albedo, and the amount of insolation from satellite measurements of radiant energy emitted by the Earth and its atmosphere. GPGS incorporates *a priori* information (initial guesses of thermodynamic parameters of the atmosphere) and radiometric measurements from the geostationary operational environmental satellites along with mathematical models of physical principles that govern the transfer of energy in the atmosphere. GPGS solves the radiative-transfer equation and provides the resulting data products in formats suitable for use by weather-forecasting computer programs. The data-assimilation capability afforded by GPGS offers the potential to improve local weather forecasts ranging from 3 hours to 2 days — especially with respect to temperature, humidity, cloud cover, and the probability of precipitation. The improvements afforded by GPGS could be of interest to news media, utility companies, and other organizations that utilize regional weather forecasts.

This program was written by Gary J. Jdlovec and Ronnie J. Suggs of Marshall Space Flight Center and Juan M. Lecue of the Universities Space Research Association and the Global Hydrology and Climate Center. For further information, contact Sammy Nabors, MSFC Commercialization Assistance Lead, at sammy.a.nabors@nasa.gov. Refer to MFS-31615.

Using Dissimilarity Metrics To Identify Interesting Designs

A computer program helps to blend the power of automated-search software, which is able to generate large numbers of design solutions, with the insight of expert designers, who are able to identify preferred designs but do not have time to examine all the solutions. From among

the many automated solutions to a given design problem, the program selects a smaller number of solutions that are worthy of scrutiny by the experts in the sense that they are sufficiently dissimilar from each other. The program makes the selection in an interactive process that involves a sequence of data-mining steps interspersed with visual displays of results of these steps to the experts. At crucial points between steps, the experts provide directives to guide the process. The program uses heuristic search techniques to identify nearly optimal design solutions and uses dissimilarity metrics defined by the experts to characterize the degree to which solutions are interestingly different. The search, data-mining, and visualization features of the program were derived from previously developed risk-management software used to support a risk-centric design methodology.

This program was written by Martin Feather of Caltech and James Kiper of Miami University, Oxford, Ohio, for NASA's Jet Propulsion Laboratory. Further information is contained in a TSP (see page 1).

This software is available for commercial licensing. Please contact Karina Edmonds of the California Institute of Technology at (626) 395-2322. Refer to NPO-40456.

X-Windows PVT Widget Class

The X-Windows Process Validation Table (PVT) Widget Class ("Class" is used here in the object-oriented-programming sense of the word) was devised to simplify the task of implementing network registration services for Information Sharing Protocol (ISP) graphical-user-interface (GUI) computer programs. Heretofore, ISP PVT programming tasks have required many method calls to identify, query, and interpret the connections and messages exchanged between a client and a PVT server. Normally, programmers have utilized direct access to UNIX socket libraries to implement the PVT protocol queries, necessitating the use of many lines of source code to perform frequent tasks. Now, the X-Windows PVT Widget Class encapsulates ISP client server network registration management tasks within the framework of an X Windows widget. Use of the widget framework enables an X Windows GUI program to interact with PVT services in an

abstract way and in the same manner as that of other graphical widgets, making it easier to program PVT clients. Wrapping the PVT services inside the widget framework enables a programmer to treat a PVT server interface as though it were a GUI. Moreover, an alternate subclass could implement another service in a widget of the same type.

This program was written by Matthew R. Barry of United Space Alliance for Johnson Space Center. For further information, contact the Johnson Technology Transfer Office at (281) 483-3809. MSC-23582

Shuttle Data Center File-Processing Tool in Java

A Java-language computer program has been written to facilitate mining of data in files in the Shuttle Data Center (SDC) archives. This program can be executed on a variety of workstations or via Web-browser programs. This program is partly similar to prior C-language programs used for the same purpose, while differing from those programs in that it exploits the platform-neutrality of Java in implementing several features that are important for analysis of large sets of time-series data. The program supports regular expression queries of SDC archive files, reads the files, interleaves the time-stamped samples according to a chosen output, then transforms the results into that format. A user can choose among a variety of output file formats that are useful for diverse purposes, including plotting, Markov modeling, multivariate density estimation, and wavelet multiresolution analysis, as well as for playback of data in support of simulation and testing.

This program was written by Matthew R. Barry and Walter H. Miller of United Space Alliance for Johnson Space Center. For further information, contact the Johnson Technology Transfer Office at (281) 483-3809. MSC-23584

Statistical Evaluation of Utilization of the ISS

PayLoad Utilization Modeler (PLUM) is a statistical-modeling computer program used to evaluate the effectiveness of utilization of the Interna-

tional Space Station (ISS) in terms of the number of research facilities that can be operated within a specified interval of time. PLUM is designed to balance the requirements of research facilities aboard the ISS against the resources available on the ISS. PLUM comprises three parts: an interface for the entry of data on constraints and on required and available resources, a database that stores these data as well as the

program output, and a modeler. The modeler comprises two subparts: one that generates tens of thousands of random combinations of research facilities and another that calculates the usage of resources for each of those combinations. The results of these calculations are used to generate graphical and tabular reports to determine which facilities are most likely to be operable on the ISS, to identify which ISS resources

are inadequate to satisfy the demands upon them, and to generate other data useful in allocation of and planning of resources.

*This program was written by Ross Andrews and Alida Andrews of Science Applications International Corp. for **Johnson Space Center**. For further information, contact the Johnson Technology Transfer Office at (281) 483-3809.
MSC-23592*



■ Nanotube Dispersions Made With Charged Surfactant

Lyndon B. Johnson Space Center, Houston, Texas

Dispersions (including monodispersions) of nanotubes in water at relatively high concentrations have been formulated as prototypes of reagents for use in making fibers, films, and membranes based on single-walled carbon nanotubes (SWNTs). Other than water, the ingredients of a dispersion of this type include one or more charged surfactant(s) and carbon nanotubes derived from the HiPco™ (or equivalent) process. Among reagents known to be made from HiPco™ (or equivalent) SWNTs, these are the most concentrated and are ex-

pected to be usable in processing of bulk structures and materials. Test data indicate that small bundles of SWNTs and single SWNTs at concentrations up to 1.1 weight percent have been present in water plus surfactant. This development is expected to contribute to the growth of an industry based on applied carbon nanotechnology. There are expected to be commercial applications in aerospace, avionics, sporting goods, automotive products, biotechnology, and medicine.

This work was done by Cynthia Kuper and Mike Kuzma of Versilant Nanotechnologies for

Johnson Space Center. For further information, contact the Technology Transfer Office at (281) 483-3809.

In accordance with Public Law 96-517, the contractor has elected to retain title to this invention. Inquiries concerning rights for its commercial use should be addressed to:

Versilant Nanotechnologies

3231 Walnut St.

Philadelphia, PA 19104

Refer to MSC-23383, volume and number of this NASA Tech Briefs issue, and the page number.

■ Aerogels for Thermal Insulation of Thermoelectric Devices

Energy-conversion efficiencies would be increased and operational lifetimes prolonged.

NASA's Jet Propulsion Laboratory, Pasadena, California

Silica aerogels have been shown to be attractive for use as thermal-insulation materials for thermoelectric devices. It is desirable to thermally insulate the legs of thermoelectric devices to suppress lateral heat leaks that degrade thermal efficiency. Aerogels offer not only high thermal-insulation effectiveness, but also a combination of other properties that are especially advantageous in thermoelectric-device applications.

Aerogels are synthesized by means of sol-gel chemistry, which is ideal for casting insulation into place. As the scale of the devices to be insulated decreases, the castability from liquid solutions becomes increasingly advantageous: By virtue of castability, aerogel insulation can be made to encapsulate devices having any size from macroscopic down to nanoscopic and possibly having complex, three-dimensional shapes. Castable aerogels can permeate voids having characteristic dimensions as small as nanometers. Hence, practically all the void space surrounding the legs of thermoelectric devices could be filled with aerogel insulation, making the insulation highly effective. Because aerogels have the lowest densities of any known solid materials, they would add very little mass to the encapsulated devices.

The thermal-conductivity values of aerogels are among the lowest reported for any material, even after taking account of the contributions of convection and radiation (in addition to true thermal conduction) to overall effective thermal conductivities. Even in ambient air, the contribution of convection to effective overall thermal conductivity of an aerogel is extremely low because of the highly tortuous nature of the flow paths through the porous aerogel structure. For applications that involve operating temperatures high enough to give rise to significant amounts of infrared radiation, opacifiers could be added to aerogels to reduce the radiative contributions to overall effective thermal conductivities. One example of an opacifier is carbon black, which absorbs infrared radiation. Another example of an opacifier is micron-sized metal flakes, which reflect infrared radiation.

Encapsulation in cast aerogel insulation also can help prolong the operational lifetimes of thermoelectric devices that must operate in vacuum and that contain SiGe or such advanced skutterudite thermoelectric materials as CoSb_3 and $\text{CeFe}_{3.5}\text{Co}_{0.5}\text{Sb}_{12}$. The primary cause

of deterioration of most thermoelectric materials is thermal decomposition or sublimation (e.g., sublimation of Sb from CoSb_3) at typical high operating temperatures. Aerogel present near the surface of CoSb_3 can impede the outward transport of Sb vapor by establishing a highly localized, equilibrium Sb-vapor atmosphere at the surface of the CoSb_3 .

This work was done by Jeffrey Sakamoto, Jean-Pierre Fleurial, Jeffrey Snyder, Steven Jones, and Thierry Caillat of Caltech for NASA's Jet Propulsion Laboratory. Further information is contained in a TSP (see page 1).

In accordance with Public Law 96-517, the contractor has elected to retain title to this invention. Inquiries concerning rights for its commercial use should be addressed to

Innovative Technology Assets Management

JPL

Mail Stop 202-233

4800 Oak Grove Drive

Pasadena, CA 91109-8099

(818) 354-2240

E-mail: iaoffice@jpl.nasa.gov

Refer to NPO-40630, volume and number of this NASA Tech Briefs issue, and the page number.

Low-Density, Creep-Resistant Single-Crystal Superalloys

Weights of aircraft turbine rotors could be reduced significantly.

John H. Glenn Research Center, Cleveland, Ohio

Several recently formulated nickel-base superalloys have been developed with excellent high-temperature creep resistance, at lower densities than those of currently used nickel-base superalloys. These alloys are the latest products of a continuing effort to develop alloys that have even greater strength-

to-weight ratios, suitable for use in turbine blades of aircraft engines. Mass densities of turbine blades exert a significant effect on the overall weight of aircraft. For a given aircraft, a reduction in the density of turbine blades enables design reductions in the weight of other parts throughout the turbine

rotor, including the disk, hub, and shaft, as well as supporting structures in the engine. The resulting total reduction in weight can be 8 to 10 times that of the reduction in weight of the turbine blades.

The approach followed in formulating these alloys involved several strategies for identifying key alloying elements and the range of concentration of each element to study. To minimize the number of alloys needed to be cast, a design-of-experiments methodology was adopted. A statistics-based computer program that models the effects of varying compositions of four elements, including effects of two-way interactions between elements, was used to test all possible alloys within the design space. The starting points for the computational analysis were three alloy compositions mandated by engineering consensus. After likewise identification of key alloying elements to vary and the allowed ranges of concentrations, the computer program then selects a minimum number of alloys within the design space to allow determination of effects for all four elements and their interactions.

On the basis of the results of the computational analysis, thirteen alloys were cast for determination of density and microstructural stability. Of these alloys, eight were cast into larger heats of single crystals and subjected to creep rupture tests at temperatures of 1,800 and 2,000 °F (982 and 1,093 °C, respectively). As shown in Figure 1, the densities of the three strongest alloys based on creep rupture were significantly lower than the density of the best second-, third-, and fourth-generation superalloys currently in use. As seen in Figure 2, the creep strength as a function of density for these various low-density superalloys was found to exceed those of the current superalloys.

In a departure from previous alloy-design practices, a conscious decision was made to sacrifice some resistance to oxidation for the sake of further optimization with respect to density and strength. This strategy involves reliance on a robust coating system for resistance to oxidation. The widespread use of coated turbine blades in engines for more than 40 years indicates this is a

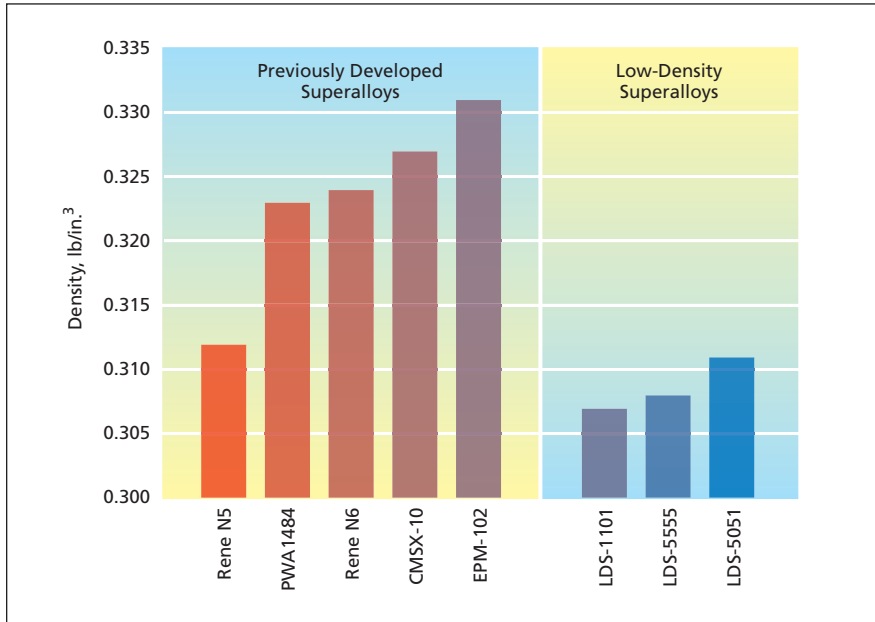


Figure 1. Measured Densities of Low-Density Superalloys are compared to previously developed superalloys.

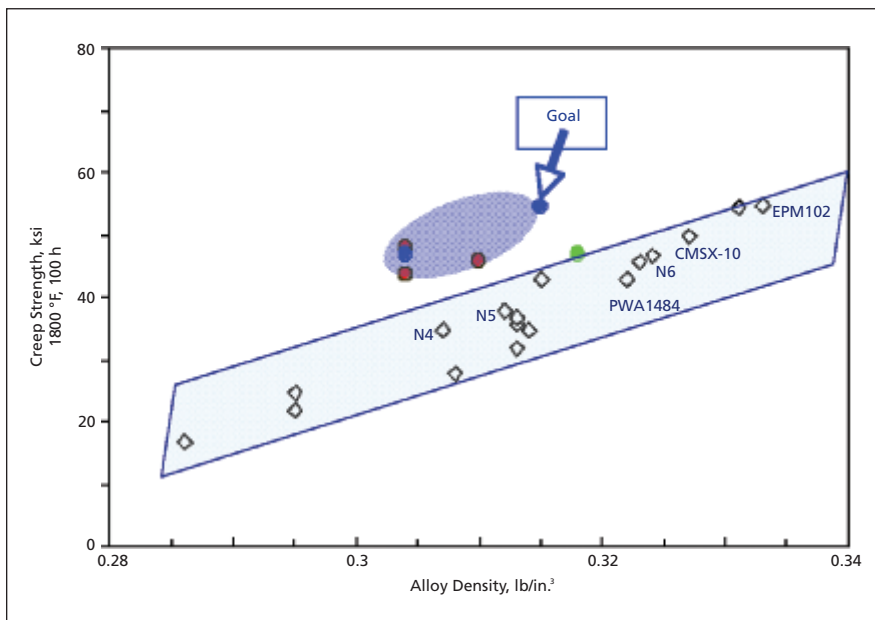


Figure 2. Past Development Approaches for first generation (Rene N4), second generation (Rene N5 and PWA1484), third generation (Rene N6 and CMSX-10), and fourth generation (EPM 102) superalloys increased alloy density with creep strength through the use of dense refractory element additions. The NASA GRC goal was to increase creep strength without concurrent increases in alloy density.

quite reasonable strategy. Nevertheless, these low-density superalloys were found to be as oxidation-resistant as that of first-generation-superalloy single crystals. Further optimization with respect to density and strength can be achieved if resistance to oxidation is

further sacrificed to an acceptable extent.

*This work was done by Rebecca A. MacKay, Timothy P. Gabb, James L. Smialek, and Michael V. Nathal of **Glenn Research Center**. Further information is contained in a TSP (see page 1).*

Inquiries concerning rights for the commercial use of this invention should be addressed to NASA Glenn Research Center, Innovative Partnerships Office, Attn: Steve Fedor, Mail Stop 4-8, 21000 Brookpark Road, Cleveland, Ohio 44135. Refer to LEW-17672-1



Excitations for Rapidly Estimating Flight-Control Parameters

Parameters are estimated, in nearly real time, from responses to these excitations.

Dryden Flight Research Center, Edwards, California

A flight test on an F-15 airplane was performed to evaluate the utility of prescribed simultaneous independent surface excitations (PreSISE) for real-time estimation of flight-control parameters, including stability and control deriva-

tives. The ability to extract these derivatives in nearly real time is needed to support flight demonstration of intelligent flight-control system (IFCS) concepts under development at NASA, in academia, and in industry. Tradition-

ally, flight maneuvers have been designed and executed to obtain estimates of stability and control derivatives by use of a post-flight analysis technique. For an IFCS, it is required to be able to modify control laws in real time for an aircraft that has been damaged in flight (because of combat, weather, or a system failure).

The flight test included PreSISE maneuvers, during which all desired control surfaces are excited simultaneously, but at different frequencies, resulting in aircraft motions about all coordinate axes. The objectives of the test were to obtain data for post-flight analysis and to perform the analysis to determine:

- The accuracy of derivatives estimated by use of PreSISE,
- The required durations of PreSISE inputs, and
- The minimum required magnitudes of PreSISE inputs.

The PreSISE inputs in the flight test consisted of stacked sine-wave excitations at various frequencies, including symmetric and differential excitations of canard and stabilator control surfaces and excitations of aileron and rudder control surfaces of a highly modified F-15 airplane. Small, medium, and large excitations were tested in 15-second maneuvers at subsonic, transonic, and supersonic speeds. Typical excitations are shown in Figure 1. Flight-test data were analyzed by use of pEst, which is an industry-standard output-error technique developed by Dryden Flight Research Center. Data were also analyzed by use of Fourier-transform regression (FTR), which was developed for onboard, real-time estimation of the derivatives.

Figure 2 shows results, for one of the derivatives, from 9 PreSISE maneuvers at Mach 0.75. At this Mach number, the airplane is statically unstable. The first set of data represents results from the use of small PreSISE inputs, the second set from medium inputs, and the third set from large inputs. For the derivative

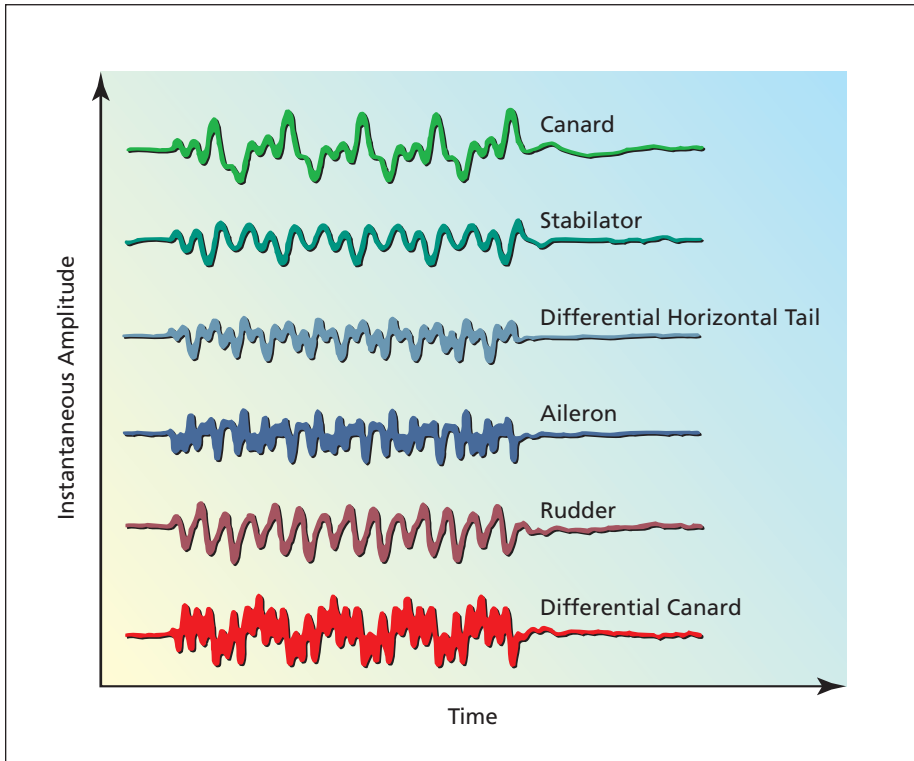


Figure 1. These **Control-Surface Excitations** were applied to an F-15 airplane to elicit responses from which stability and control derivatives could be estimated.

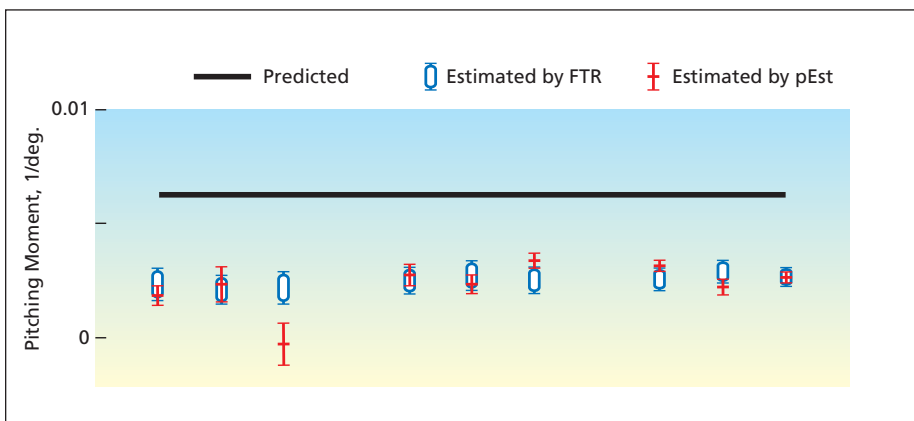


Figure 2. A **Pitching Moment** due to the angle of attack was predicted and was estimated from responses to PreSISE at small, medium, and large magnitudes.

in question, the estimate was the same, independent of input size or analysis technique. Typically, the longitudinal derivatives were estimated with acceptably high accuracy and, using FTR, converged to final values after about 5 seconds of inputs. Some lateral-directional

derivatives were not estimated as accurately, because signal-to-noise ratios were low. Efforts to optimize the inputs for increased accuracy in estimation of the derivatives are underway.

This work was done by Tim Moes and Mark Smith of Dryden Flight Research

Center and Gene Morelli of Langley Research Center. For further information, contact Mr. Moes at (661) 276-3054, Mr. Smith at (661) 276-3177, or Mr. Morelli at (757) 864-4078.

DRC-03-06

✈ Estimation of Stability and Control Derivatives of an F-15

Parameters can be estimated in nearly real time for use in adaptive flight control.

Dryden Flight Research Center, Edwards, California

A technique for real-time estimation of stability and control derivatives (derivatives of moment coefficients with respect to control-surface deflection angles) was used to support a flight demonstration of a concept of an indirect-adaptive intelligent flight control system (IFCS). Traditionally, parameter identification, including estimation of stability and control derivatives, is done post-flight. However, for the indirect-adaptive IFCS concept, parameter identification is required during flight so that the system can modify control laws for a damaged aircraft.

The flight demonstration was carried out on a highly modified F-15 airplane (see Figure 1). The main objective was to estimate the stability and control derivatives of the airplane in nearly real time. A secondary goal was to develop a system to automatically assess the quality of the results, so as to be able to tell a learning neural network which data to use.

Parameter estimation was performed by use of Fourier-transform regression (FTR) — a technique developed at NASA Langley Research Center. FTR is an equation-error technique that operates in the frequency domain. Data are put into the frequency domain by use of a recursive Fourier transform for a discrete frequency set. This calculation simplifies many subsequent calculations, removes biases, and automatically filters out data beyond the chosen frequency range.

FTR as applied here was tailored to work with pilot inputs, which produce



Figure 1. The F-15 #837 Airplane was used in a flight demonstration of the real-time parameter-estimation technique.

correlated surface positions that prevent accurate parameter estimates, by replacing half the derivatives with predicted values. FTR was also set up to work only on a recent window of data, to accommodate changes in flight condition.

A system of confidence measures was developed to identify quality-parameter estimates that a learning neural network could use. This system judged the estimates primarily on the basis of their estimated variances and of the level of aircraft response.

The resulting FTR system was implemented in the Simulink software system and autocoded in the C programming language for use on the Airborne Research Test System (ARTS II) computer installed in the F-15 airplane. The Simulink model was also used in a control room that utilizes the Ring Buffered Network Bus hardware and software, making it possible to evaluate test points during flights.

In-flight parameter estimation was done for piloted and automated maneuvers, pri-

marily at three test conditions. Figure 2 shows results for pitching moment due to symmetric stabilator actuations for a series of three pitch doublet maneuvers (in a doublet maneuver, a command to change attitude in a given direction by a given amount is followed immediately by a command to change attitude in the opposite direction by the same amount). A time window of 5 seconds was used. The portions of the curves shown in red are those that passed the confidence tests.

The technique showed good convergence for most derivatives for both kinds of maneuvers — typically within a few seconds. The confidence tests were marginally successful, and it would be necessary to refine them for use in an IFCS.

This work was done by Mark Smith and Tim Moes of Dryden Flight Research Center and Gene Morelli of Langley Research Center. For further information, contact Mark Smith at (661) 276-3177, Tim Moes at (661) 276-3054, or Gene Morelli at (757) 864-4078.

DRC-03-05

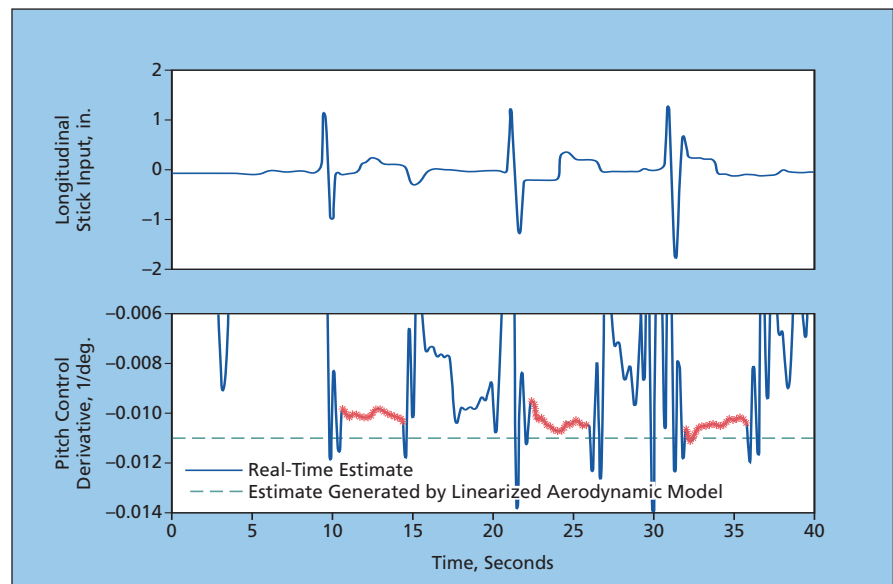


Figure 2. These Results Derived From a Pitching-Moment Test involving three pitch-doublet maneuvers illustrate the capability afforded by the real-time parameter-estimation technique.

Tool for Coupling a Torque Wrench to a Round Cable Connector

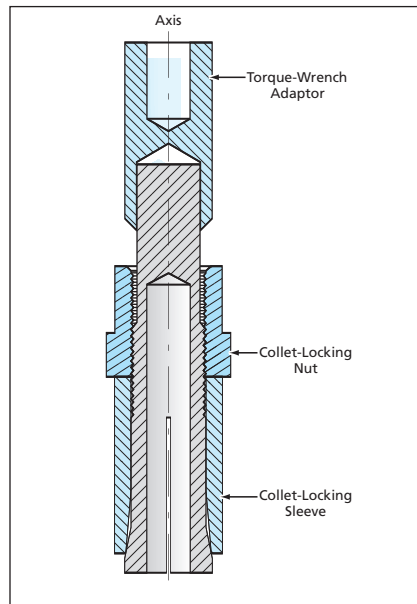
Torque is applied without offset.

Lyndon B. Johnson Space Center, Houston, Texas

A tool makes it possible to couple a torque wrench to an externally knurled, internally threaded, round cable connector. The purpose served by the tool is to facilitate the tightening of multiple such connectors (or the repeated tightening of the same connector) to repeatable torques.

The design of a prior cable-connector/torque-wrench coupling tool provided for application of the torque-wrench jaws to a location laterally offset from the axis of rotation of the cable connector, making it necessary to correct the torque reading for the offset. Unlike the design of the prior tool, the design of the present tool provides for application of the torque-wrench jaws to a location on the axis of rotation, obviating correction of the torque reading for offset.

The present tool (see figure) consists of a split collet containing a slot that provides clearance for inserting and bending the cable, a collet-



This **Simple Tool** makes it possible to tighten round cable connectors to repeatable torques, without need to make offset corrections.

locking sleeve, a collet-locking nut, and a torque-wrench adaptor that is press-fit onto the collet. Once the collet is positioned on the cable connector, the collet-locking nut is turned to force the collet-locking sleeve over the collet, compressing the collet through engagement of tapered surfaces on the outside of the collet and the inside of the locking sleeve. Because the collet is split and therefore somewhat flexible, this compression forces the collet inward to grip the connector securely. The torque wrench is then applied to the torque-wrench adaptor in the usual manner for torquing a nut or a bolt.

This was done by Scott C. Hacker, Richard J. Dean, and Scott W. Burge of Johnson Space Center. For further information, contact Johnson Technology Transfer Office at (281) 483-3809.



Ultrasonically Actuated Tools for Abrading Rock Surfaces

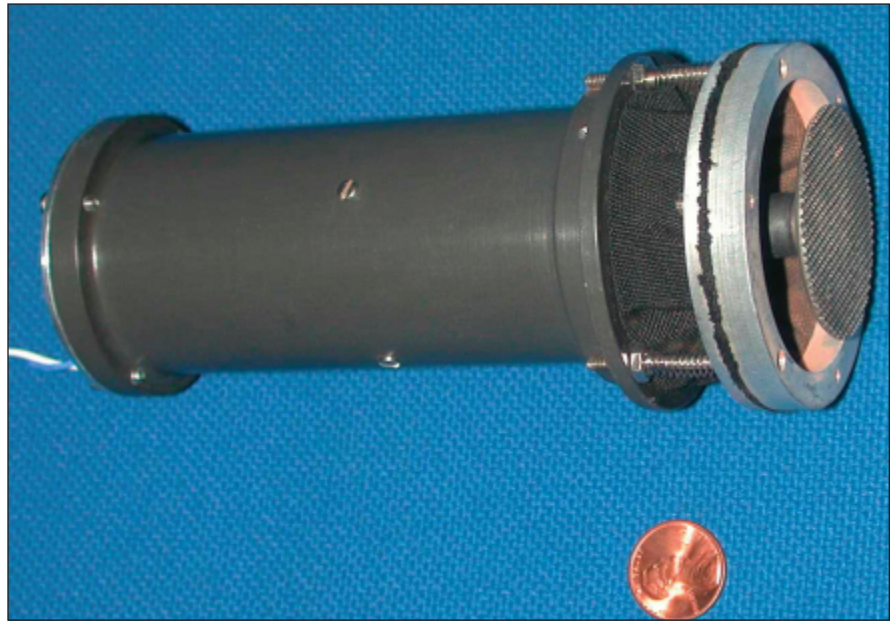
These offer the same advantages as do ultrasonically actuated drilling and coring tools.

NASA's Jet Propulsion Laboratory, Pasadena, California

An ultrasonic rock-abrasion tool (URAT) was developed using the same principle of ultrasonic/sonic actuation as that of the tools described in two prior *NASA Tech Briefs* articles: "Ultrasonic/Sonic Drill/Corers With Integrated Sensors" (NPO-20856), Vol. 25, No. 1 (January 2001), page 38 and "Ultrasonic/Sonic Mechanisms for Drilling and Coring" (NPO-30291), Vol. 27, No. 9 (September 2003), page 65. Hence, like those tools, the URAT offers the same advantages of low power demand, mechanical simplicity, compactness, and ability to function with very small axial loading (very small contact force between tool and rock).

Like a tool described in the second of the cited previous articles, a URAT includes (1) a drive mechanism that comprises a piezoelectric ultrasonic actuator, an amplification horn, and a mass that is free to move axially over a limited range and (2) an abrasion tool bit. A URAT tool bit is a disk that has been machined or otherwise formed to have a large number of teeth and an overall shape chosen to impart the desired shape (which could be flat or curved) to the rock surface to be abraded. In operation, the disk and thus the teeth are vibrated in contact with the rock surface. The concentrated stresses at the tips of the impinging teeth repeatedly induce microfractures and thereby abrade the rock. The motion of the tool induces an ultrasonic transport effect that displaces the cuttings from the abraded area.

The figure shows a prototype URAT. A piezoelectric-stack/horn actuator is housed



This **Prototype URAT** is one of several that have been constructed thus far. It has a total mass of 0.4 kg, a length of 5.65 in. (14.4 cm), and a maximum diameter of 2.5 in. (6.35 cm). The textured disk at the right end is the tool bit.

in a cylindrical container. The movement of the actuator and bit with respect to the housing is aided by use of mechanical sliders. A set of springs accommodates the motion of the actuator and bit into or out of the housing through an axial range between 5 and 7 mm. The springs impose an approximately constant force of contact between the tool bit and the rock to be abraded. A dust shield surrounds the bit, serving as a barrier to reduce the migration of rock debris to sensitive instrumentation or mechanisms in the vicinity. A bushing at

the tool-bit end of the housing reduces the flow of dust into the actuator and retains the bit when no axial load is applied.

This work was done by Benjamin Dolgin, Stewart Sherrit, Yoseph Bar-Cohen, Richard Rainen, Steve Askin, Donald Bickler, Donald Lewis, John Carson, Stephen Dawson, Xiaoqi Bao, and Zensheu Chang of Caltech and Thomas Peterson of Cybersonics for NASA's Jet Propulsion Laboratory. Further information is contained in a TSP (see page 1). NPO-30403

Active Struts With Variable Spring Stiffness and Damping

These struts would act as linear actuators and controllable shock absorbers.

Langley Research Center, Hampton, Virginia

Controllable active struts that would function as linear actuators with variable spring stiffness and damping have been proposed as components of advanced suspension systems of future wheeled

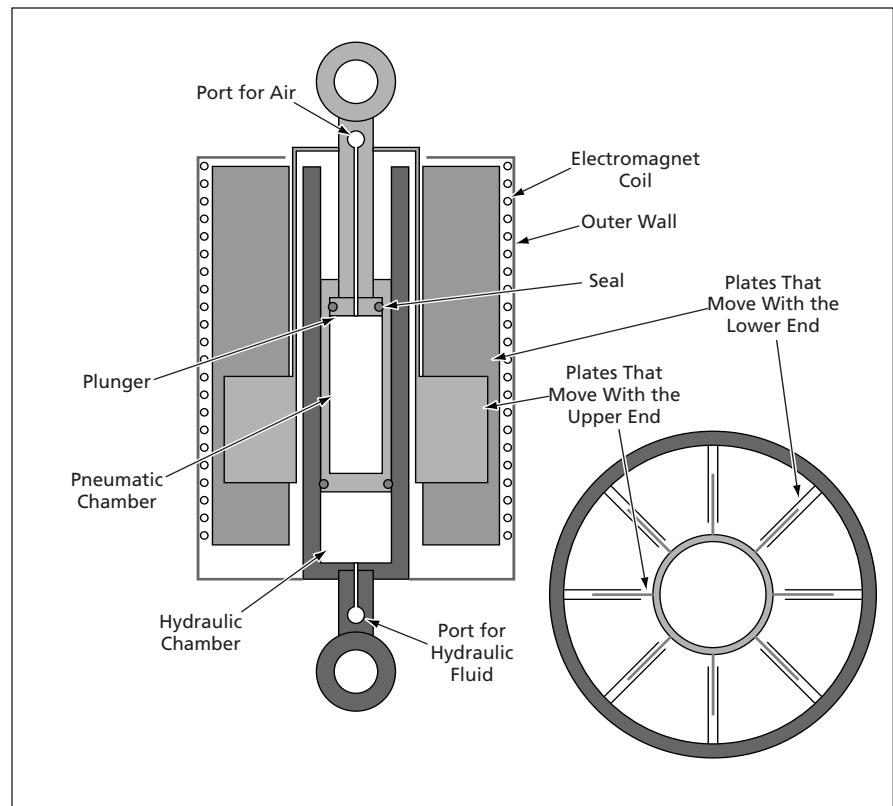
ground vehicles. The contemplated advanced suspension systems would include computer-based control subsystems that would continually adjust the actuator responses to obtain optimal

combinations of safety and comfort under operating conditions ranging from low speeds over smooth roads to high speeds over rough, unpaved ground. The proposed struts and suspen-

sion systems were originally intended for use in military vehicles, but there could also be a broad commercial market for them in trucks and sport utility vehicles.

A strut according to the proposal (see figure) would include an air spring in the form of a plunger sliding longitudinally in a pneumatic chamber. Compressed air would be supplied to the pneumatic chamber, from an external pump and accumulator, via a pneumatic hose and a high-speed valve. The chamber would be instrumented with (1) an electronic extensometer to monitor the axial displacement of the plunger and (2) an electronic air-pressure sensor. Notwithstanding the extensometer, the air spring would be used primarily to regulate the spring stiffness, rather than the length, of the strut. The diameter of the plunger would be small, so that only a small amount of compressed air would have to be pumped in or allowed to flow out to change the spring stiffness by a given amount. Because of the small amount of air needed and because the air spring would operate at moderate to high pressure, the required amount of air could be made to flow into or out of it rapidly and, hence, the spring stiffness could be changed rapidly on command.

The pneumatic chamber would also serve as a plunger that would slide longitudinally in a hydraulic chamber. Like the pneumatic chamber, the hydraulic chamber would be equipped with a pressure sensor, extensometer, and high-speed valve. However, instead of compressed air, hydraulic fluid would be supplied to this chamber from an external hydraulic pump, accumulator, and reservoir. The hydraulic chamber would be used primarily to adjust the length of the strut; secondarily, it could be used as a very stiff spring in the event of a malfunction of the air spring. The hydraulic fluid would be pumped in to extend the strut. Retraction would be effected by actuating the valve to allow the load on the strut to push hydraulic fluid back to the reservoir. Like the pneumatic chamber,



A **Strut Assembly** according to the proposal would contain a pneumatic actuator, a hydraulic actuator, and a magnetorheological damping actuator.

the hydraulic chamber would have a small volume and would be operated at high pressure; hence, the length of the strut could be adjusted within a short response time.

A device denoted an actuator-restraining device (ARD) would provide controllable damping. The ARD would include (1) a set of plates, oriented in radial-axial planes, that would move with one end of the strut and (2) a set of pairs of plates, each pair parallel and close to one of the first-mentioned plates, that would move with the other end of the strut. The narrow spaces between the plates would be filled with a magnetorheological fluid, the effective viscosity of which would be controlled by the current in an electromagnet coil. In the absence of current, the plates would slide almost freely, so

that any damping would be that attributable to friction damping in the air spring and the hydraulic actuator. In general, the amount of damping could be increased or decreased to almost any desired level by increasing or decreasing the current applied to the coil. By applying sufficient current, one could even obtain a damping or restraining force greater than the weight of the vehicle. The response time of the ARD would be an order of magnitude shorter than the response times of the pneumatic and hydraulic actuators.

*This work was done by Gary L. Farley of the U. S. Army Research Laboratory for **Langley Research Center**. Further information is contained in a TSP (see page 1). LAR-16355-1*



Multi-axis, Lightweight, Computer-Controlled Exercise System

This system offers unprecedented versatility for physical conditioning and evaluation.

Lyndon B. Johnson Space Center, Houston, Texas

The multipurpose, multi-axis, isokinetic dynamometer (MMID) is a computer-controlled system of exercise machinery that can serve as a means for quantitatively assessing a subject's muscle coordination, range of motion, strength, and overall physical condition with respect to a wide variety of forces, motions, and exercise regimens. The MMID is easily reconfigurable and compactly stowable and, in comparison with prior computer-controlled exercise systems, it weighs less, costs less, and offers more capabilities.

Whereas a typical prior isokinetic exercise machine is limited to operation in

only one plane, the MMID can operate along any path. In addition, the MMID is not limited to the isokinetic (constant-speed) mode of operation. The MMID provides for control and/or measurement of position, force, and/or speed of exertion in as many as six degrees of freedom simultaneously; hence, it can accommodate more complex, more nearly natural combinations of motions and, in so doing, offers greater capabilities for physical conditioning and evaluation.

The MMID (see figure) includes as many as eight active modules, each of which can be anchored to a floor, wall,

ceiling, or other fixed object. A cable is payed out from a reel in each module to a bar or other suitable object that is gripped and manipulated by the subject. The reel is driven by a DC brushless motor or other suitable electric motor via a gear reduction unit. The motor can be made to function as either a driver or an electromagnetic brake, depending on the required nature of the interaction with the subject. The module includes a force and a displacement sensor for real-time monitoring of the tension in and displacement of the cable, respectively. In response to commands from a control computer, the motor can be operated to generate a required tension in the cable, to displace the cable a required distance, or to reel the cable in or out at a required speed.

The computer can be programmed, either locally or via a remote terminal, to support exercises in one or more of the usual exercise modes (isometric, isokinetic, or isotonic) along complex, multi-axis trajectories. The motions of, and forces applied by, the subject can be monitored in real time and recorded for subsequent evaluation. Through suitable programming, the exercise can be adjusted in real time according to the physical condition of the subject. The remote-programming capability makes it possible to connect multiple exercise machines into a network for supervised exercise by multiple subjects or even for competition by geographically dispersed subjects.

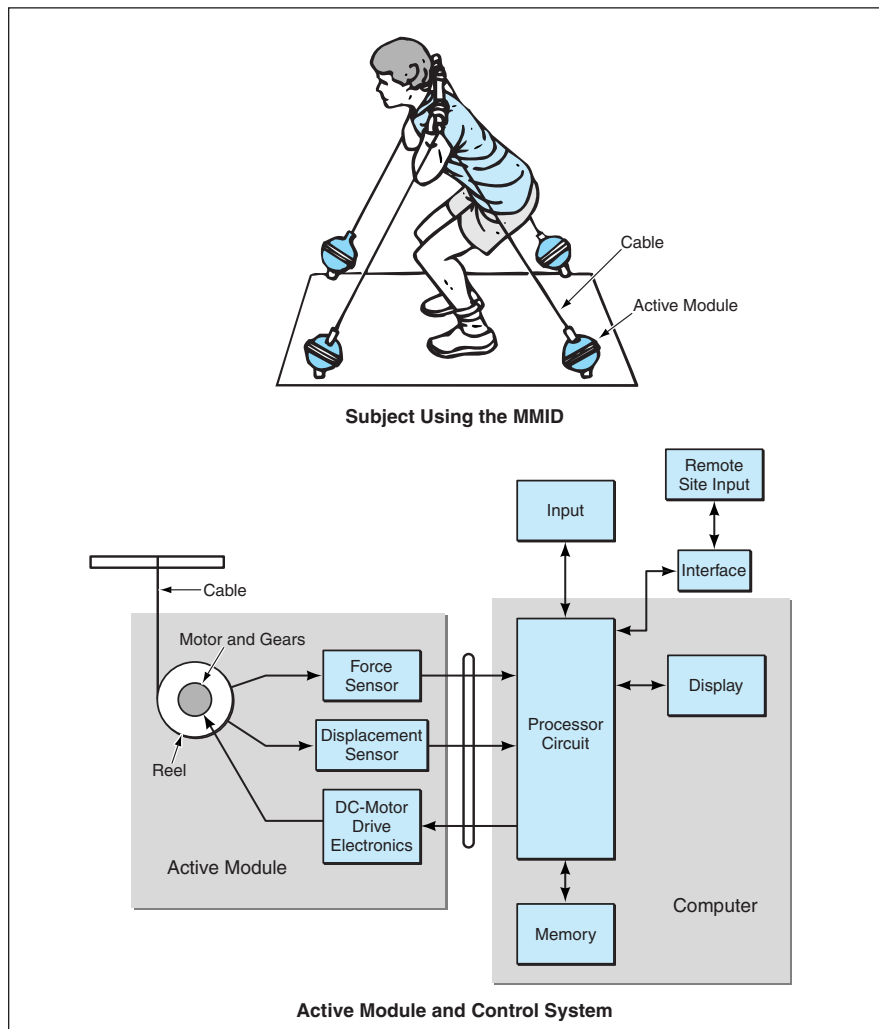
This work was done by Leonard Haynes, Benjamin Bachrach, and William Harvey of Intelligent Automation, Inc., for Johnson Space Center.

In accordance with Public Law 96-517, the contractor has elected to retain title to this invention. Inquiries concerning rights for its commercial use should be addressed to:

*Intelligent Automation
7519 Standish Place, Suite 200
Rockville, MD 20855
Phone: (301) 294-5200*

Web site: <http://www.i-a-i.com>

Refer to MSC-23353, volume and number of this NASA Tech Briefs issue, and the page number.



Computer-Controlled Active Modules pay out or retract cables at controlled tension, displacement, or speed.

Dehydrating and Sterilizing Wastes Using Supercritical CO₂

Lyndon B. Johnson Space Center, Houston, Texas

A relatively low-temperature process for dehydrating and sterilizing biohazardous wastes in an enclosed life-support system exploits (1) the superior mass-transport properties of supercritical fluids in general and (2) the demonstrated sterilizing property of supercritical CO₂ in particular. The wastes to be treated are placed in a chamber. Liquid CO₂, drawn from storage at a pressure of 850 psi (≈5.9 MPa) and temper-

ature of 0 °C, is compressed to pressure of 2 kpsi (≈14 MPa) and made to flow into the chamber. The compression raises the temperature to 10 °C. The chamber and its contents are then further heated to 40 °C, putting the CO₂ into a supercritical state, in which it kills microorganisms in the chamber. Carrying dissolved water, the CO₂ leaves the chamber through a back-pressure regulator, through which it is ex-

panded back to the storage pressure. The expanded CO₂ is refrigerated to extract the dissolved water as ice, and is then returned to the storage tank at 0 °C.

*This work was done by Ian J. Brown of Lynntech, Inc. for **Johnson Space Center**. For further information, contact the Johnson Technology Transfer Office at (281) 483-3809. MSC-23495*



Alpha-Voltaic Sources Using Liquid Ga as Conversion Medium

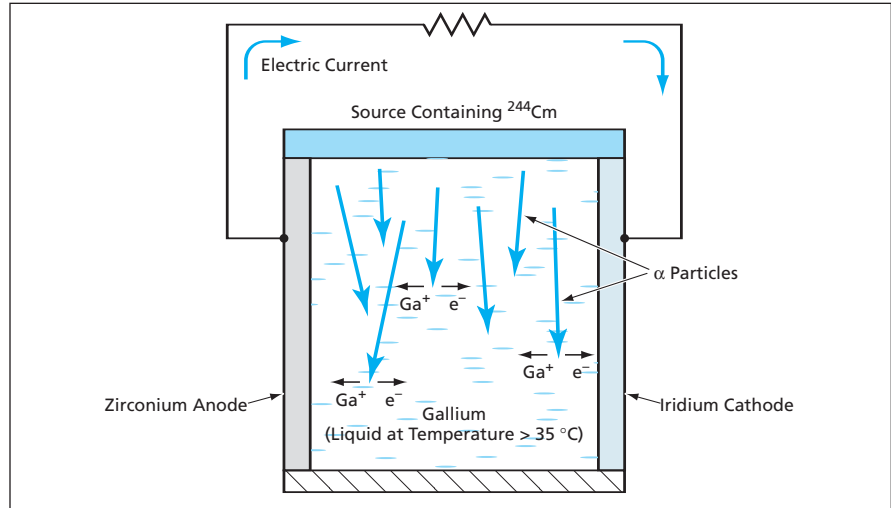
These units would offer long life and high energy-conversion efficiency.

NASA's Jet Propulsion Laboratory, Pasadena, California

A family of proposed miniature sources of power would exploit the direct conversion of the kinetic energy of α particles into electricity. In addition to having long operational lives, these sources are expected to operate with energy-conversion efficiencies from 70 to 90 percent.

A power source as proposed (see figure) would be an electrolytic cell in which liquid gallium would serve as both an electrolyte and an energy-conversion medium. The cell would contain an iridium cathode and a zirconium anode. The α particles, each with a kinetic energy ~ 5.8 MeV, would be emitted by radioactive decay of ^{244}Cm , which has a half-life of 18 years. The ^{244}Cm source would be positioned so that the α particles would enter the liquid gallium, where their kinetic energy would be dissipated mostly through ionization of Ga atoms, creating Ga^+ ions and free electrons. The electrons would be collected by iridium cathode, and the Ga^+ ions would be neutralized at the zirconium cathode by electrons returning after flowing through an external circuit.

Gallium is a candidate for use as the electrolyte and the energy-conversion medium because in the liquid state it is a semimetal: its electrical conductivity is greater than that of a typical semiconductor but small in comparison with the conductivities of metals. Consequently, in liquid gallium, electrons and Ga^+ can exist without immediate recombination and can be moved by electric fields. It is expected that electric fields, resulting at least partly from the difference between



Liquid Gallium in an Electrolytic Cell would be ionized by impinging α particles. The resulting electric charges would be collected at the electrodes.

the work functions of the electrode metals, would move the electrons and ions to their respective electrodes. The open-circuit potential of the cell is expected to be 1.62 V — equal to the difference between the work functions of iridium and zirconium.

Unlike in a solid-state energy conversion medium, the impingement of energetic α particles would not give rise to displacement damage in the liquid gallium. Hence, the cell should have a long life, limited only by the half-life of ^{244}Cm . A cell having a volume less than 25 mm³, containing 1 curie of ^{244}Cm (the curie is a unit of radioactivity equal to 3.7×10^{10} disintegrations per second)

is expected to deliver a current between 7 and 12 mA, which, at the expected open-circuit potential, would provide a power in the approximate range of 11 to 20 mW.

This work was done by Jagdish U. Patel, Jean-Pierre Fleuriel, and G. Jeffrey Snyder of Caltech for NASA's Jet Propulsion Laboratory. Further information is contained in a TSP (see page 1).

This invention is owned by NASA, and a patent application has been filed. Inquiries concerning nonexclusive or exclusive license for its commercial development should be addressed to the Patent Counsel, NASA Management Office-JPL at (818) 354-7770. Refer to NPO-30322.

Ice-Borehole Probe

The art of borehole imaging has been extended to deep, cold, wet, high-pressure environments.

NASA's Jet Propulsion Laboratory, Pasadena, California

An instrumentation system has been developed for studying interactions between a glacier or ice sheet and the underlying rock and/or soil. Prior borehole imaging systems have been used in well-drilling and mineral-exploration

applications and for studying relatively thin valley glaciers, but have not been used for studying thick ice sheets like those of Antarctica.

The system includes a cylindrical imaging probe that is lowered into a hole

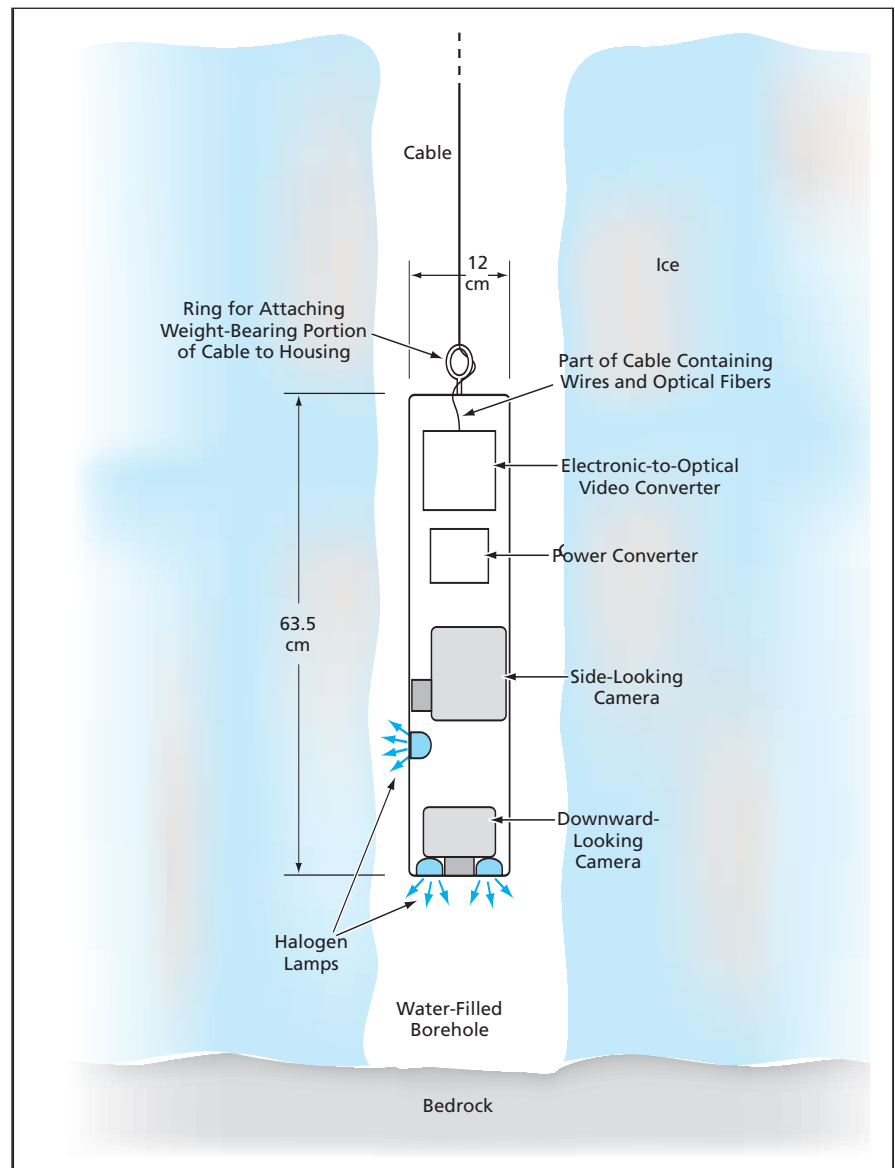
that has been bored through the ice to the ice/bedrock interface by use of an established hot-water-jet technique. The images acquired by the cameras yield information on the movement of the ice relative to the bedrock and on

visible features of the lower structure of the ice sheet, including ice layers formed at different times, bubbles, and mineralogical inclusions. At the time of reporting the information for this article, the system was just deployed in two boreholes on the Amery ice shelf in East Antarctica and after successful 2000–2001 deployments in 4 boreholes at Ice Stream C, West Antarctica, and in 2002 at Black Rapids Glacier, Alaska.

The probe is designed to operate at temperatures from -40 to $+40$ °C and to withstand the cold, wet, high-pressure [130-atm (13.20-MPa)] environment at the bottom of a water-filled borehole in ice as deep as 1.6 km. A current version is being outfitted to service 2.4-km-deep boreholes at the Rutford Ice Stream in West Antarctica. The probe (see figure) contains a side-looking charge-coupled-device (CCD) camera that generates both a real-time analog video signal and a sequence of still-image data, and contains a digital videotape recorder. The probe also contains a downward-looking CCD analog video camera, plus halogen lamps to illuminate the fields of view of both cameras. The analog video outputs of the cameras are converted to optical signals that are transmitted to a surface station via optical fibers in a cable. Electric power is supplied to the probe through wires in the cable at a potential of 170 VDC. A DC-to-DC converter steps the supply down to 12 VDC for the lights, cameras, and image-data-transmission circuitry. Heat generated by dissipation of electric power in the probe is removed simply by conduction through the probe housing to the adjacent water and ice.

One of the new, creative, and very important attributes of this system is its ability to provide the scientist/operator with direct real-time imaging of the ice in front of the cameras. This allows real-time interaction of a knowledgeable observer and control over when to stop to study further, as well as the two-way command and control that lets one zoom/focus into the ice structure to get “internal” versus wall-structure views at a 100- to 200-mm scale.

The probe is lowered into the borehole by using the cable as a tether. The cable is 1.6 km long and is wound on a spool about 0.9 m in diameter. The spool is rotated by a three-phase AC motor to pay out or pull in the cable at a speed of about 1 m/s. In addition to the wires for transmitting power and the optical fibers for transmitting data,



A Cylindrical Probe Housing containing two cameras is lowered to the bottom of a borehole in ice to acquire images of ice structures, inclusions, and ice/bedrock interactions.

the cable contains strengthening members and includes a waterproof cover. The cable, the spool, the motor, and a sled on which the spool and motor are mounted have a total mass of 180 kg. Other equipment in the surface station includes the following: two video monitors that display the current video feeds from each camera; two digital video tape recorders that digitize the incoming analog video images and store the resulting data for subsequent analysis; and a computer that is used to control the operation of the probe and, after image data have been acquired, to digitally manipulate the images and analyze their contents.

All the image data are time-tagged to enable detailed correlations of images

during *post factum* analysis. To assist an operator in subsequently locating unique image features, the real-time video display contains subwindows that indicate depth and time. The highest-quality digital images are recorded by a digital videotape recorder within the side-looking camera. The videotape is removed from the probe after the probe has been returned to the surface station. Time tagging provides a direct correlation between these taped images and the ones recorded in the surface station.

This work was done by Alberto Behar, Frank Carsey, Arthur Lane, and Herman Engelhardt of Caltech for NASA's Jet Propulsion Laboratory. Further information is contained in a TSP (see page 1). NPO-40500

Alpha-Voltaic Sources Using Diamond as Conversion Medium

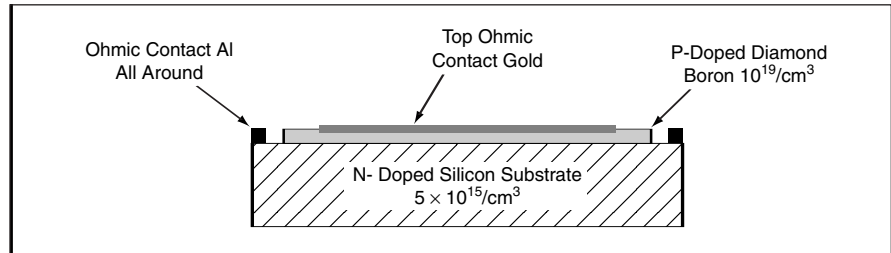
Compact, long-lived solid-state devices would tolerate wide temperature ranges.

NASA's Jet Propulsion Laboratory, Pasadena, California

A family of proposed miniature sources of power would exploit the direct conversion of the kinetic energy of α particles into electricity in diamond semiconductor diodes. These power sources would function over a wide range of temperatures encountered in terrestrial and outer-space environments. These sources are expected to have operational lifetimes of 10 to 20 years and energy conversion efficiencies >35 percent.

A power source according to the proposal would include a pair of devices like that shown in the figure. Each device would contain Schottky and p/n diode devices made from high-band-gap, radiation-hard diamond substrates. The n and p layers in the diode portion would be doped sparsely ($<10^{14} \text{ cm}^{-3}$) in order to maximize the volume of the depletion region and thereby maximize efficiency. The diode layers would be supported by an undoped diamond substrate.

The source of α particles would be a thin film of ^{244}Cm (half-life 18 years) sand-



This **Diamond Diode** is one of two that would be sandwiched together with a thin film of ^{244}Cm , which is a source of α particles. The sandwich structure would constitute an alpha-voltaic device.

wiched between the two paired devices. The sandwich arrangement would force almost every α particle to go through the active volume of at least one of the devices. Typical α particle track lengths in the devices would range from 20 to 30 microns. The α particles would be made to stop only in the undoped substrates to prevent damage to the crystalline structures of the diode portions.

The overall dimensions of a typical source are expected to be about 2 by 2 by 1 mm. Assuming an initial ^{244}Cm mass of 20 mg, the estimated initial out-

put of the source is 20 mW (a current of 20 mA at a potential of 1 V).

This work was done by Jagdish U. Patel, Jean-Pierre Fleuriel, and Elizabeth Kolawa of Caltech for NASA's Jet Propulsion Laboratory. Further information is contained in a TSP (see page 1).

This invention is owned by NASA, and a patent application has been filed. Inquiries concerning nonexclusive or exclusive license for its commercial development should be addressed to the Patent Counsel, NASA Management Office-JPL at (818) 354-7770. Refer to NPO-30323.

White-Light Whispering-Gallery-Mode Optical Resonators

Overlapping resonator modes are exploited to obtain wide, high-Q spectra.

NASA's Jet Propulsion Laboratory, Pasadena, California

Whispering-gallery-mode (WGM) optical resonators can be designed to exhibit continuous spectra over wide wavelength bands (in effect, white-light spectra), with ultrahigh values of the resonance quality factor (Q) that are nearly independent of frequency. White-light WGM resonators have potential as superior alternatives to (1) larger, conventional optical resonators in ring-down spectroscopy, and (2) optical-resonator/electro-optical-modulator structures used in coupling of microwave and optical signals in atomic clocks. In these and other potential applications, the use of white-light WGM resonators makes it possible to relax the requirement of high-frequency stability of lasers, thereby enabling the use of cheaper lasers.

In designing a white-light WGM resonator, one exploits the fact that the density of the mode spectrum increases predictably with the thickness of the

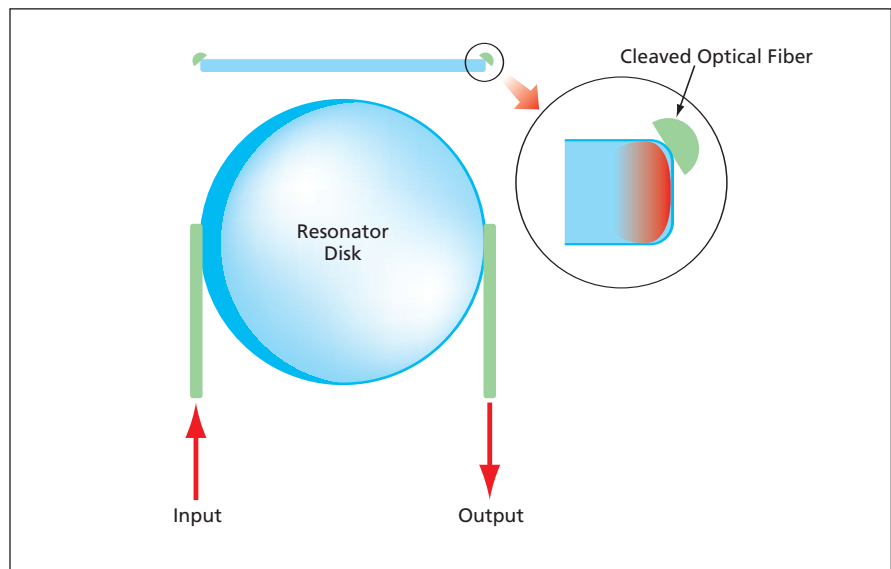


Figure 1. **Cleaved Optical Fibers** tangential to the rim of the resonator disk are used to couple light into and out of the disk. The fibers are shifted with respect to the middle of the rim to obtain a high degree of interaction with all the WGM modes.

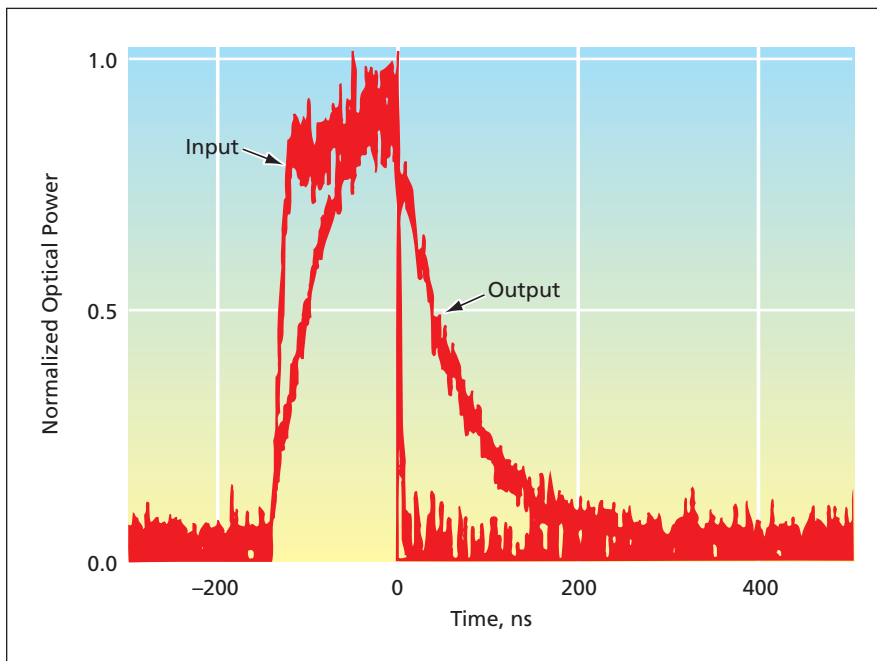


Figure 2. **Normalized Power Levels** of input and output pulses of light, as functions of time, were determined in the setup depicted in Figure 1. The small amplitude modulation in the ring-down tail was attributed to slight non-preservation of orthogonality between resonator modes — an artifact of the input/output coupling technique.

resonator disk. By making the resonator disk sufficiently thick, one can make the frequency differences between adjacent modes significantly less than the spectral width of a single mode, so that the spectral peaks of adjacent modes overlap, making the resonator spectrum essentially continuous. Moreover, inasmuch as the Q values of the various modes are deter-

mined primarily by surface Rayleigh scattering that does not depend on mode numbers, all the modes have nearly equal Q . By use of a proper coupling technique, one can ensure excitation of a majority of the modes.

For an experimental demonstration of a white-light WGM resonator, a resonator disk 0.5-mm thick and 5 mm in diameter was made from CaF_2 . The

shape of the resonator and the fiber-optic coupling arrangement were as shown in Figure 1. The resonator was excited with laser light having a wavelength of 1,320 nm and a spectral width of 4 kHz. The coupling efficiency exceeded 80 percent at any frequency to which the laser could be set in its tuning range, which was >100-GHz wide.

The resonator response was characterized by means of ring-down tests in which the excitation was interrupted by a shutter having a rise and a fall time of 5 ns. The ring-down time of photodiodes and associated circuitry used to measure the interrupted excitation and the resonator output was <1 ns. Figure 2 shows the shapes of representative input and output light pulses. The average ring-down time was found to be 120 ns, corresponding to $Q \approx 2 \times 10^8$. The variations of Q with the laser carrier frequency were found to be <5 percent. Hence, the resonator was shown to have the desired “white light” properties.

This work was done by Andrey Matsko, Anatoliy Savchenkov, and Lute Maleki of Caltech for NASA’s Jet Propulsion Laboratory. Further information is contained in a TSP (see page 1).

This invention is owned by NASA, and a patent application has been filed. Inquiries concerning nonexclusive or exclusive license for its commercial development should be addressed to the Patent Counsel, NASA Management Office–JPL. Refer to NPO-42221.



Books & Reports

Controlling Attitude of a Solar-Sail Spacecraft Using Vanes

A paper discusses a concept for controlling the attitude and thrust vector of a three-axis stabilized Solar Sail spacecraft using only four single degree-of-freedom articulated spar-tip vanes. The vanes, at the corners of the sail, would be turned to commanded angles about the diagonals of the square sail. Commands would be generated by an adaptive controller that would track a given trajectory while rejecting effects of such disturbance torques as those attributable to offsets between the center of pressure on the sail and the center of mass. The controller would include a standard proportional + derivative part, a feedforward part, and a dynamic component that would act like a generalized integrator. The controller would globally track reference signals, and in the presence of such control-actuator constraints as saturation and delay, the controller would utilize strategies to cancel or reduce their effects. The control scheme would be embodied in a robust, nonlinear algorithm that would allocate torques among the vanes, always finding a stable solution arbitrarily close to the global optimum solution of the control effort allocation problem. The solution would include an acceptably small angle, slow limit-cycle oscillation of the vanes, while providing overall thrust vector pointing stability and performance.

This work was done by Edward Mettler, Ahmet Acikmese, and Scott Ploen of Caltech for NASA's

Jet Propulsion Laboratory. *Further information is contained in a TSP (see page 1).*

The software used in this innovation is available for commercial licensing. Please contact Karina Edmonds of the California Institute of Technology at (626) 395-2322. Refer to NPO-42156.

Wire-Mesh-Based Sorber for Removing Contaminants From Air

A paper discusses an experimental regenerable sorber for removing CO₂ and trace components — principally, volatile organic compounds, halocarbons, and NH₃ — from spacecraft cabin air. This regenerable sorber is a prototype of what is intended to be a lightweight alternative to activated-carbon and zeolite-pellet sorbent beds now in use. The regenerable sorber consists mainly of an assembly of commercially available meshes that have been coated with a specially-formulated washcoat containing zeolites. The zeolites act as the sorbents while the meshes support the zeolite-containing washcoat in a configuration that affords highly effective surface area for exposing the sorbents to flowing air. The meshes also define flow paths characterized by short channel lengths to prevent excessive buildup of flow boundary layers. Flow boundary layer resistance is undesired because it can impede mass and heat transfer. The total weight and volume comparison versus the atmosphere revitalization

equipment used onboard the International Space Station for CO₂ and trace-component removal will depend upon the design details of the final embodiment. However, the integrated mesh-based CO₂ and trace-contaminant removal system is expected to provide overall weight and volume savings by eliminating most of the trace-contaminant control equipment presently used in parallel processing schemes traditionally used for spacecraft. The mesh-based sorbent media enables integrating the two processes within a compact package. For the purpose of regeneration, the sorber can be heated by passing electric currents through the metallic meshes combined with exposure to space vacuum. The minimal thermal mass of the meshes offers the potential for reduced regeneration-power requirements and cycle time required for regeneration compared to regenerable sorption processes now in use.

This work was done by Jay Perry of Marshall Space Flight Center, and Subir Roychoudhury and Dennis Walsh of Precision Combustion, Inc.

In accordance with Public Law 96-517, the contractor has elected to retain title to this invention. Inquiries concerning rights for its commercial use should be addressed to:

Precision Combustion, Inc.

410 Sackett Point Road

North Haven, CT 06473-3106

Phone No.: (203) 287-3700

Fax No.: (203) 287-3710

Refer to MFS-32308-1, volume and number of this NASA Tech Briefs issue, and the page number.



National Aeronautics and
Space Administration